



5-2013

Soil Microbial Community Succession During Cadaver Decomposition

Kelly Lynn Cobaugh

University of Tennessee - Knoxville, kcobaugh@utk.edu

Recommended Citation

Cobaugh, Kelly Lynn, "Soil Microbial Community Succession During Cadaver Decomposition." Master's Thesis, University of Tennessee, 2013.

https://trace.tennessee.edu/utk_gradthes/1604

This Thesis is brought to you for free and open access by the Graduate School at Trace: Tennessee Research and Creative Exchange. It has been accepted for inclusion in Masters Theses by an authorized administrator of Trace: Tennessee Research and Creative Exchange. For more information, please contact trace@utk.edu.

To the Graduate Council:

I am submitting herewith a thesis written by Kelly Lynn Cobaugh entitled "Soil Microbial Community Succession During Cadaver Decomposition." I have examined the final electronic copy of this thesis for form and content and recommend that it be accepted in partial fulfillment of the requirements for the degree of Master of Science, with a major in Environmental and Soil Sciences.

Jennifer M. DeBruyn, Major Professor

We have read this thesis and recommend its acceptance:

Amy Z. Mundorff, Sean M. Schaeffer, Shawn A. Hawkins

Accepted for the Council:

Dixie L. Thompson

Vice Provost and Dean of the Graduate School

(Original signatures are on file with official student records.)

Soil Microbial Community Succession During Cadaver
Decomposition

A Thesis Presented for the
Master of Science
Degree
The University of Tennessee, Knoxville

Kelly Lynn Cobaugh
May 2013

Copyright © 2013 by Kelly Lynn Cobaugh
All rights reserved.

ACKNOWLEDGEMENTS

Firstly, I would like to express my gratitude the members of my Thesis Committee, especially Dr. Jennifer DeBruyn, for their guidance throughout this process. This study would not have been accomplished if not for the support of the UT ARF: thank you to Dr. Lee Meadows Jantz, Dr. Rebecca Taylor, Jake Smith, and Yangseung Jeong. A special thank you to Kathleen Hauther and my undergraduate student helpers, Mikhail Androsov and Kristen Shara, for their assistance in laboratory tasks and soil sampling. Also, I would like to thank Dan Williams and Dr. Alice Layton of the UT Center for Biotechnology who provided the HuBac plasmid and their assistance with the HuBac qPCR assay, and Dr. Bonnie Ownley of the UT Entomology and Plant Pathology department who provided the fungal DNA. To my labmates, Xiaoci Ji, Alex Bevard, Mariam Fawaz and Chelsea Delay, for their help in one way or another. To Peter Tonner who generously donated his computer programming and editing skills. And lastly, and most importantly, to my parents: I am so fortunate to have their unconditional support in all of my endeavors.

ABSTRACT

Microbes play critical roles in nutrient cycling in terrestrial ecosystems. In particular, microbial decomposition of organic matter is a key step in carbon and nutrient cycling, linking above-ground and below-ground pools. It is well known that the microbial community changes in structure and function following the introduction of organic matter into a terrestrial system. The decomposition of plant litter has been extensively investigated but the decomposition of animal-derived organic matter has often been overlooked. The unique characteristics of animal input are hypothesized to dictate a distinct decomposition process. This study examined the microbial community responsible for decomposition of animal-derived organic matter. Our objective was to determine the taxonomic and functional succession of microbial populations in a Cadaver Decomposition Island (CDI) during decomposition. To address our objectives, soils from beneath four cadavers at the UT Anthropological Facility were sampled throughout the decomposition process. Reproducible patterns in the concentration of extractable total nitrogen, ammonia and organic carbon in the soil were observed. The distinct trends in microbial respiration and net N mineralization rates indicated that a major functional shift in the community occurred following the Active Decay stage. Human-associated *Bacteroides* were detected at high concentrations throughout decomposition, up to 198 days after cadavers were first placed. This study revealed the succession in microbial community function and structure during decomposition of animal-derived organic matter, and has implications in the fields of public health and forensic science.

PREFACE

“We tend to train our attention and science on life and growth, but of course death and decomposition are no less important to nature’s operations ...” (Pollan 2006).

Microbial ecology has long been separated conceptually from the ecology of macrobiota. But as investigation continues on their survival strategies and interactions, we are starting to see some unifying principles across the divisions of life. We are also starting to realize their importance in nutrient cycling, generation of economically important secondary metabolites and enzymes (Karlovsky 2008), and their ability to degrade contaminants (Lee Wise 2000). We have only just scratched the surface of the ‘black box’ (it will take some time to study the estimated 10^4 - 10^9 bacterial species on Earth!). This study investigates the microbes responsible for a key soil process: decomposition. Extensive study has been done on the decomposition of fertilizer and plant organic matter, but we barely know anything about animal organic matter. Below is a brief review of studies on the microbial decomposition of plant matter, which give us a framework for understanding animal organic matter as an important part of the organic matter pool and global biogeochemical cycles.

TABLE OF CONTENTS

Table of Contents

CHAPTER I Literature Review	1
Microbial Nutrient Cycling in Soils.....	1
Soil Organic Matter.....	2
Decomposition of Animal-Derived Organic Matter	3
Basic processes in animal decomposition.....	3
Hot Spots and Hot Moments.....	4
Biological Invasion	6
Building a Cell	7
Stoichiometry Rules.....	7
Microbial Life Histories.....	8
Bacterial-Fungal Interactions.....	9
Why Microbial Diversity Matters	10
CHAPTER II Objectives and Hypotheses	12
Objective 1	12
Hypothesis 1.....	12
Rationale	12
Hypothesis 2.....	12
Rationale	12
Approach.....	12
Objective 2	12
Hypothesis 1.....	13
Rationale	13
Hypothesis 2.....	14
Rationale	14
Approach.....	14
CHAPTER III Materials and Methods	15
Study Design.....	15
Site Description.....	15
Climate.....	15
Study Location Within the ARF	16
Soil Sampling.....	18
Normalization for Temperature Differences.....	19
Soil Characteristics	19
Soil Moisture Content.....	19
Soil Chemistry	19
pH.....	19
Microbial Activity.....	20
Microbial Biomass Production	20
Microbial Respiration	20
Microbial Growth Efficiency.....	21
DNA Extraction and Preparation	21

DNA Extraction	21
DNA Quantification.....	22
Quantitative PCR (qPCR).....	22
Creation of Bacterial 16S Plasmid for qPCR Standard	22
Quantification of Bacterial 16S rRNA genes.....	23
Quantification of Human-Associated Bacteriodes.....	23
Quantification of Fungal ITS Region	24
Statistical Analysis.....	25
Binning.....	25
Statistical Tests	25
CHAPTER IV Results	27
Bacterial biomass production rates	27
Microbial Respiration	32
Microbial Growth Efficiency	36
Nitrogen Fractions	37
Net N Mineralization	39
Extractable Organic Carbon.....	40
Extractable Phosphate.....	41
pH.....	42
Human-Associated Bacteriodes 16S rRNA Abundances via qPCR.....	43
Total Bacterial 16S and Fungal ITS region rRNA Abundances via qPCR	44
CHAPTER V Discussion and Conclusions	45
Summary.....	51
LIST OF REFERENCES	52
APPENDIX.....	65
Vita.....	67

LIST OF TABLES

Table 1. Summary of Life History Strategies	9
Table 2. Metadata associated with cadavers placed in this study	18
Table 3. Summary of mean and standard deviations from all CDI data. Asterisk (*) indicates value was significantly above respective control value using the Wilcoxon Signed Rank Test ($p < 0.05$). A double asterisk (**) indicates value was significantly above initial value using the Wilcoxon Rank Sum test ($p < 0.05$)	28
Table 4. Variables that were significantly correlated with Spearman Rank-Order Correlation coefficients (r_s) > 0.50	30
Table A1. Decomposition stage at each sampling day. The sample code is the cadaver number followed by the day after placement.....	66

LIST OF FIGURES

Figure 1. Simplified schematic of decomposition in N cycle. Figure taken from Schimel et al. (2004)	1
Figure 2. The operational stages of carcass decomposition.....	3
Figure 3. Breakdown of cadaveric protein, figure taken from Dent et al. (2004)	4
Figure 4. Variation in community structure between vertebrate gut-associated (green) and free-living bacterial communities (red), as in the soil. Taken from Ley et al. (2008) 6	
Figure 5. Relative abundances of phyla in 16S rRNA gene libraries from a variety of ecosystems. Boxed in black are soil (left) and gut (right) communities. Figure adapted from Ley et al. (2008).....	10
Figure 6. Hypothesized response curves of the two main microbial assemblages in CDI soils: carcass associated microflora (blue) and a succession of soil opportunists (green).	13
Figure 7. Aerial view of UT Anthropological Research Facility (Photo credit: Google Maps)	15
Figure 8. Density of cadaver placement from 2001-2005 at the ARF, Demann (2010). Placement of cadavers from the current study is marked in red.	17
Figure 9. Difference in bacterial biomass production between cadaver decomposition island (CDI) soils for four cadavers (36, 47, 50, 67) and control soils, estimated from leucine incorporation rates in bacterial suspensions extracted from soil. Data is presented by cumulative degree hours (CDH).....	29
Figure 10. Correlation between leucine incorporation rates and total 16S rRNA gene copies ($r_s=0.8225$, $p<0.001$).	31
Figure 11. Soil respiration rates during a 48 hour incubation at room temperature (mg CO ₂ -C per hour per gram dry weight (gdw)) as a function of the cumulative degree hours (CDH) in soils beneath cadavers and their respective control samples.	32
Figure 12. Data presented in Figure 11 is here shown for just the Bloat and Active Decay stages. Data is presented by cumulative degree hours (CDH).....	33
Figure 13. Correlation between total extractable organic carbon and microbial respiration ($r_s= 0.5847$, $p<0.001$).	34
Figure 14. Correlation between total extractable nitrogen and microbial respiration ($r_s=0.6390$, $p<0.001$).	35
Figure 15. Microbial growth efficiency, calculated as biomass production rate divided by the sum of biomass production rate and respiration rate, during the different stages of decomposition. Abbreviation key as follows: Bloat-Act (Bloat-Active), Act (Active), Initial Adv (Initial Advanced Decay), Adv I (Advanced Decay I), Adv II (Advanced Decay II), Adv III (Advanced Decay III).....	36
Figure 16. Extractable Nitrogen fractions of cadaver decomposition island (CDI) soils during decomposition compared to total nitrogen concentrations in the control soils. Abbreviation key as follows: Bloat-Act (Bloat-Active), Act (Active), Initial Adv (Initial Advanced Decay), Adv I (Advanced Decay I), Adv II (Advanced Decay II), Adv III (Advanced Decay III).....	38

Figure 17. Net N mineralization in cadaver decomposition island (CDI) soils and their respective control soils (a) #36, (b) #47, (c) #50, and (d) #67. Data is presented by cumulative degree hours (CDH). 39

Figure 18. Total extractable organic carbon (EOC) in cadaver decomposition island (CDI) and control soils during decomposition. Abbreviation key as follows: Bloat-Act (Bloat-Active), Act (Active), Initial Adv (Initial Advanced Decay), Adv I (Advanced Decay I), Adv II (Advanced Decay II), Adv III (Advanced Decay III). 40

Figure 19. Extractable phosphate concentrations in the cadaver decomposition island (CDI) soils and control soils. Abbreviation key as follows: Bloat-Act (Bloat-Active), Act (Active), Initial Adv (Initial Advanced Decay), Adv I (Advanced Decay I), Adv II (Advanced Decay II), Adv III (Advanced Decay III). 41

Figure 20. pH in cadaver decomposition island (CDI, filled symbols) and respective control soils (open symbols) for (a) #36, (b) #47, (c) #50, and (d) #67. Data is presented by cumulative degree hours (CDH). 42

Figure 21. Human-associated *Bacteroides* 16S rRNA gene abundances in soil underneath cadavers (a) #36, (b) #47, (c) #50, and (d) #67. Data is presented by cumulative degree hours (CDH). 43

CHAPTER I LITERATURE REVIEW

Microbial Nutrient Cycling in Soils

An important, often overlooked occupation in any community (even a microbial one!) is waste management. Saprophytic microorganisms, such as bacteria and fungi, play this key role in recycling organic residue into below and above ground pools of nutrients. They target dead organic material (detritus) or existing recalcitrant soil organic matter (SOM) for their energy, carbon and nitrogen needs. In a terrestrial ecosystem, detritus is usually a variety of plant litter and animal carcasses. Depolymerization is the critical, often rate-limiting, step from detritus polymers to something bioavailable (Figure 1). This step releases bioavailable monomers such as amino acids, lignin, starch, lipids, nucleic acids etc. for immediate use by plants or microbes. Studies suggest that even in high nitrogen conditions, extracellular enzymes are still excreted by microbes to depolymerize complex detritus to 'mine' C and N (an often limiting element in soil ecosystems) (Jans-Hammermeister et al. 1997; Fontaine et al. 2003).

When N is not limited, microbial metabolism can mineralize monomeric organic compounds to inorganic forms like ammonium (NH_4), phosphate (H_2PO_4^-), and sulfate (SO_4^{2-}). When ammonium is abundant, it can be transformed into nitrate through nitrification, a two-step process. First, ammonium is oxidized to nitrite by specific obligate aerobes like *Aerobacter aerogenes*, *Streptomyces griseus* and a variety of *Pseudomonas*

species; oxygen must be present for nitrifiers to conduct ammonia oxidation, but some have the capacity to slowly respire with nitrite as the final electron acceptor (Robertson & P. Groffman 2007).

Second, nitrite is oxidized into nitrate by the α , δ and γ Proteobacteria subclasses,

Nitrobacter, *Nitrospina*, *Nitrospira* and *Nitrococcus* (Robertson & P. Groffman 2007).

Besides the lack of oxygen, nitrification can be inhibited by low pH, and high chloride concentrations (Johnson 1992). Nitrate is a strong acid anion and high concentrations lead to acidification of soil, and depletion of minerals like Ca^{2+} and Mg^{2+} (Likens et al. 2013). Also, nitrate is more susceptible to leaching than ammonium (does not adsorb to negative clay particles) and could cause health effects if it contaminates the groundwater

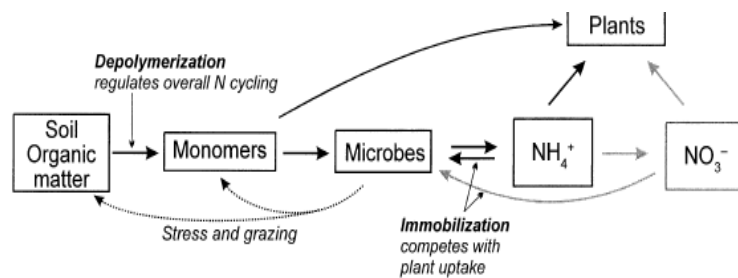


Figure 1. Simplified schematic of decomposition in N cycle. Figure taken from Schimel et al. (2004)

(Rail 2000). Nitrate can also be lost via denitrification to nitrous oxide and then dinitrogen gas. Any of the inorganic forms of N mentioned above can be stored as plant and microbial biomass (immobilization), although there is some evidence that plants in a variety of ecosystems can uptake organic N forms like amino acids (Joshua P Schimel & Chapin F. Stuart 1996). Upon cell death, microbial cellular components such as lipids, amino sugars and cell walls, can be recycled back into the pool of organic N polymers.

The strongest factor that dictates the speciation of inorganic nitrogen is the concentration of oxygen. In an anoxic (anaerobic) system, the inorganic N speciation is dominated by ammonium since nitrification is limited. Generally, when oxygen is not present, facultative aerobes must use another terminal electron acceptor, like NO_3^- , Fe (III), Mn (IV) etc., with a lower potential energy yield than oxygen. If an inorganic electron acceptor is not available, glucose can act as an electron donor and acceptor during fermentation. Both processes yield less energy compared to aerobic respiration thus anaerobic metabolism slows down decomposition (Tate 1979). Even in oxic, well-drained soils, pockets (<1 centimeter) of anoxic 'microsites' allow anaerobic processes, like fermentation or anaerobic respiration, to occur (Parkin 1987). These anoxic microsites can arise from limited water diffusion, or high local respiration from new detritus deposits (Parkin 1987). Opposing redox processes could be only millimeters away (G. van der Lee et al. 1999). Despite their small size, microsites can contribute greatly to the total activity of a local ecosystem (Parkin 1987).

The contribution of microbes to nutrient cycling on a landscape scale is not limited to the nitrogen cycle: microbes balance plant CO_2 fixation (in photosynthesis) by respiring CO_2 back into the atmosphere as they decompose detritus and/or SOM. The turnover of carbon from recent plant residue varies from 10 years in tropical savannas and grasslands to 520 years in wetlands (this is why they are such good C sinks!) (Raich & Schlesinger 1992). In contrast, carbon in recalcitrant SOM are protected by clay aggregates and can remain for thousands of years (Paul et al. 2001). To complete the terrestrial C cycle, over time and pressure the organic material buried in soil and sediments may become fossil fuels, such as coal and oil. When these are burned, carbon is returned back into the atmosphere.

Soil Organic Matter

The formation and decay of SOM is important to the biochemical and physical properties of soil and therefore, the health of soil microbial communities and plant growth. Microbial byproducts of metabolism will complex into recalcitrant, heterogeneous, amorphous mixtures of polysaccharides, melanin, proteins, plant and microbial lipids, nucleic acids, etc. These 'humic substances' (a major part of SOM) associate with soil minerals and amorphous oxides to form complexes that contribute to aggregate stability. These organo-mineral complexes also improve aeration, nutrient/water flux, and temperature retention capacity. Soil microbes benefit from the additional habitats created by improved soil structure. SOM buffers soil pH, increases cation exchange capacity (CEC) and complexes metal cations and nonionic organic compounds (Essington 2004; Horwath 2007).

The input of new labile litter does not mean that recalcitrant SOM is ignored as a nutrient source: new litter deposition is often associated with the increased decomposition

of the SOM already present (Fontaine et al. 2004). This phenomenon could be explained by an increase in SOM-degrading populations subsidized by the increased bioavailability of energy/C from the litter, or there could be a general increase in exoenzyme production. This is called the ‘priming effect’ (Fontaine et al. 2003). The decomposition of this older SOM is also affected by soil texture and water potential. In contrast, climate and C:N:P ratio affect decomposition of new plant litter (Berg & McClaugherty 2008; Scott 1996). The drivers of animal carcass decomposition will be discussed in a subsequent section. SOM is retained better in a soil with more clay than a soil with a higher sand content (Horwath 2007; Jenkinson 1977), although local climate and organic matter input might be factors as well (Müller & Höper 2004).

Decomposition of Animal-Derived Organic Matter

Basic processes in animal decomposition

While carcass/cadaver decomposition on the soil surface is not a process with distinct stages, it helps to categorize common phenomena for investigational purposes. While the terminology and number of stages varies, most researchers in the field adopted Payne’s 1965 division of decomposition into five stages: Fresh, Bloat, Active Decay, Advanced Decay, and Dry/Remains

(summarized in Figure 2). The assignment of stages relies on a combination of the larval development stage of blowfly species and the characteristics of the cadaver. Variables that affect decay rates of carcasses and human cadavers include temperature, rainfall, humidity, trauma, burial depth and soil pH (Mann et al. 1990).

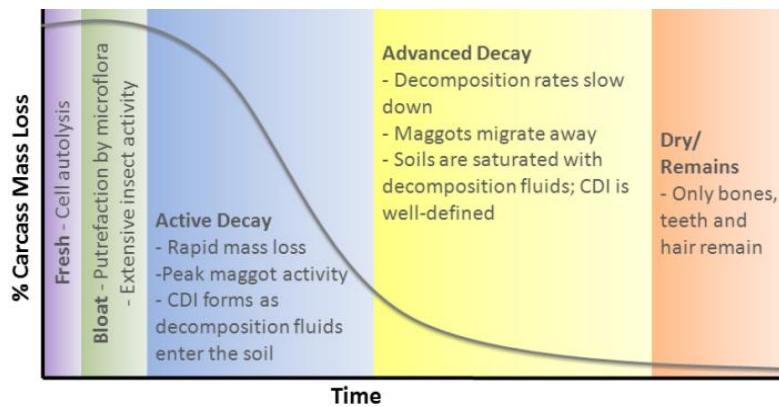


Figure 2. The operational stages of carcass decomposition.

It only takes four minutes after death for decomposition to begin: oxygen depletes, carbon dioxide levels increase, and pH decreases, killing the animal’s cells. As a cell dies, the lysosomes release enzymes, like proteases and DNases, which dissolve the insides, and eventually break the membrane causing this fluid to spill into the body cavity (Vass et al. 2002). After enough autolysis, the process of putrefaction can begin. Putrefaction is the widespread digestion of human tissue by enteric microorganisms. Due to the depletion of oxygen levels, the cavity becomes completely anaerobic and creates an

ideal environment for the proliferation of enteric bacteria originating from the gut- one of the largest bacterial communities in the body (Vass et al. 2002). Sometimes, this is first marked by a green discoloration of the lower abdomen. At this stage, anaerobic (and incomplete aerobic) decomposition will release organic acids, alcohols and acetate as fermentation byproducts, which will start to demineralize the bone, leaching calcium and phosphate into the cavity (Child 1995). Sulfur-containing amino acids are reduced to produce hydrogen sulfide and ammonia. Hydrogen sulfide and iron form a black precipitant in the capillaries near the skin surface: this is referred to as ‘marbling’. Released gases, such as carbon dioxide, methane, ammonia, and sulfur dioxide, will bloat the body cavity- deforming it until it splits open (Vass et al. 2002).

At this point, a diverse set of compounds leach into the soil. These include adipose tissues; volatile fatty acids (primarily butyric and propionic acids); organic acids, like acetic acid and oxalic acid, derived from oxaloacetic acid from the Krebs cycle; organic nitrogen from nucleic acids and proteins; amino acids from muscle decomposition, and phenolics (Vass et al. 1992). Also, aerobic bacteria from the soil are presumably introduced into the cadaver (Vass et al. 2002; Dent et al. 2004). Active Decay is characterized by cadaver mass loss due to purging of fluid/gas into the surrounding environment, and continued decomposition by microorganisms and blowfly larvae. When the larvae have migrated away from the cadaver to the pupate stage, this signals the start of Advanced Decay (Howard et al. 2010). Initial skeletalization and mummification of the body is seen in this phase.

The transition from Advanced Decay to Dry/Remains stage has no conclusive definition but more bones are continually exposed as the severely desiccated tissue disintegrates (Payne 1965; Carter & Tibbett 2008). Figure 3 summarizes the breakdown from cadaver biomolecules, such as protein, to biomass and respiratory gases. Even after skeletonization, elevated soil concentrations of total nitrogen, ammonium and phosphorus still persist even up to three years post-mortem (Hopkins et al. 2000; Towne 2000; Parmenter & MacMahon 2009).

Hot Spots and Hot Moments

Previous discussion of decomposition in terrestrial ecosystems has mostly focused on plant litter as detritus, since most studies to date have focused solely on this input. But dead organic residue can be animal-derived (like carcasses, excrement etc.) too. Animal-derived organic matter is chemically and physically distinct from plant-derived organic matter,

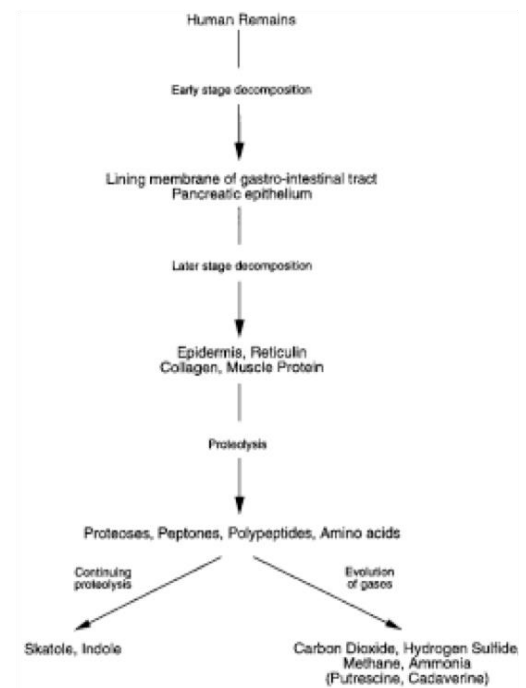


Figure 3. Breakdown of cadaveric protein, figure taken from Dent et al. (2004)

resulting in unique decomposition process dynamics. Mammal carcasses have a narrow carbon to nitrogen ratio (5:1-8:1), high water content, and a wider variety of nutrients and faster decomposition rates than plant litter (Parmenter & MacMahon 2009). As much as 5,000 kg per year of carcasses can be introduced to a square kilometer of a terrestrial ecosystem, as in the case of large ungulates in prairie ecosystems; they also contribute to landscape heterogeneity and biodiversity (Carter et al. 2007; Parmenter & MacMahon 2009).

The deposition of an animal carcass creates a fertility island. The term “fertility island” was first coined in 1970 by Garcia-Moya et al. (1970) to describe a phenomenon of nitrogen and other nutrient accumulation around/beneath shrubs in arid and semiarid ecosystems. The resulting landscape heterogeneity is probably from the shrubs’ (usually legumes) ability to attract animal activity and form a symbiotic relationship with nitrogen fixers, and/or eluvium and alluvium deposits (wind and water transported soil) (Ridolfi et al. 2008; Perroni-Ventura et al. 2010). Forensic scientists and terrestrial ecologists have adapted the fertility island concept to describe the fact that a cadaver or carcass creates a similar localized ecosystem as a result of the intense pulses of nutrients and organic matter flowing into the area; they call these newly created areas ‘**cadaver (or carcass) decomposition islands (CDIs)**’ (Carter et al. 2007). The result of this input is an area of biogeochemical cycling that is disproportionately higher than its surroundings- this is known as a "hot spot" (Parkin 1987). If biogeochemical cycling increases for a short time span, it produces a "hot moment" (McClain et al. 2003). Indeed, previous studies have noted increases in microbial respiration (Carter & Tibbett 2008; Hopkins et al. 2000; A. S. Wilson et al. 2007), and biomass production (Carter & Tibbett 2008; Hopkins et al. 2000) underneath carcasses. A CDI is clearly an overlapping of a hot spot and a hot moment.

The CDI can be seen shortly after Active Decay stage as a darkening of the soil underneath and surrounding the body, presumably from the purge fluid. The size of the CDI is determined by the mass of the cadaver, maggot quantity and the soil texture beneath the cadaver. During Advanced Decay and Dry/Remains stages, vegetation death in and around the CDI is often seen. Possible causes include: nitrogen toxicity, and /or suffocation by the cadaver (Carter et al. 2007). In contrast, immediately outside the CDI, increased plant growth can be seen (Carter et al. 2007). The spatial area of elevated total organic carbon (TOC) and nitrogen (TON) from the CDI is larger than other compounds associated with grave soils such as phosphate, sulfate, calcium etc. (Aitkenhead-Peterson et al. 2012).

Biological Invasion

To complicate matters, the hot spot and hot moment of a CDI are accompanied by a biological invasion. In this case, the ‘invaders’ are the commensal microflora associated with the cadaver. This is a very distinct community compared to that of the soil (Figure 4) (Ley et al. 2008). Over a trillion microorganisms (estimates range from 10^{11} to 10^{14} per gram of wet weight) live in the human gut, helping it to break down otherwise indigestible foods, and providing its host with vitamins, such as Vitamin B and K (Gill et al. 2006; Hill 1997). These microbes are purged into the soil with the rest of the bodily fluids following the Bloat stage.

To the author’s knowledge, no study has examined a soil invasion of an entire bacterial community. If the effects of an invasive plant pathogenic fungus are any indication, the cascading repercussions could be great: disrupting symbiosis, changing decomposition pattern and introducing pathogen resistance (which could threaten the plant species and possibly affect the microbial community) (Van der Putten et al. 2007). Without any literature, we can only review macro-scale biological invasion concepts and speculate on possible requirements for invader persistence using articles on genetically modified bacterium release.

Historically, the term ‘invasive’ has taken on a negative connotation. Since the impact on the indigenous community is unknown in this study, we will define an invasion as the proliferation of any non-indigenous species in a new geographical location (Desprez-Loustau et al. 2007). For any species to survive, they must exploit a novel niche or utilize resources more efficiently than the current dominant population. The dispersal and proliferation of pathogenic bacteria from a cadaver is of concern for public health if they are capable of reaching the groundwater. Thankfully, surface charges on clay particles and OM adsorb microbes and tortuous soil structure, like that of clayey soils, retards microbial diffusion by slowing the water infiltration (Marshall 1971). But a slope of 10% or more was shown to increase the risk of dispersal (Rahe 1978). High pH is also favorable to transport: twice as many bacteria were retained in the soil matrix of a microcosm at a pH of three instead of six (Bitton et al. 1974).

The combination of a CDI and biological invasion can be looked at as a ‘disturbance’ to the current ecosystem. Not to be confused with the term ‘stress’, a disturbance is an isolated pulse that disrupts the ecosystem, community or population; this could change the physical environment or resource availability (McClain et al. 2003). Instead, stress is usually a chronic state, like drought, freezing, changes in salinity/pH etc.

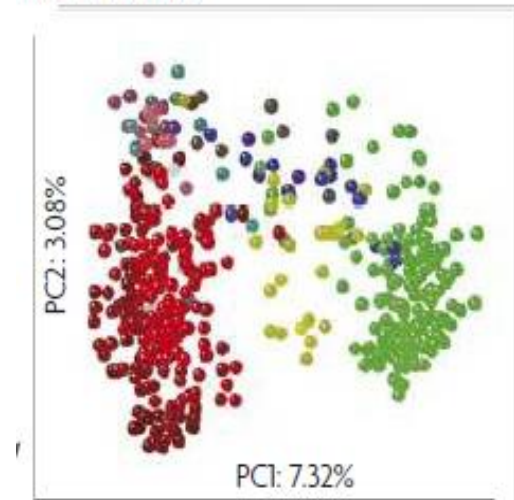


Figure 4. Variation in community structure between vertebrate gut-associated (green) and free-living bacterial communities (red), as in the soil. Taken from Ley et al. (2008)

(J. P. Schimel et al. 2007). It has been shown that most microbial groups are sensitive to disturbances such as elevated CO₂, mineral fertilization, abrupt temperature changes and C amendments- all of which are present when a cadaver is introduced to the environment (Vass et al. 1992; A. S. Wilson et al. 2007; Allison & Martiny 2008).

Building a Cell

Understanding a microbial community's nutrient requirements is key to the study of decomposition. While their nutrient utilization is complex, unifying principles have emerged. When detritus is introduced into an ecosystem, microbes have to produce exoenzymes to break down the complex compounds of the litter. Depending on their need, 10–20% of total biomass production can be devoted to this exoenzyme production (J. Schimel & Weintraub 2003). This concept of having to 'spend money to make money' is a risky enterprise for microbes: if they do not get a return on their investment (amount of nutrients/energy returned is less than the energy cost to produce the enzymes) growth would stop and the organism could starve. Often times, labile compounds from root exudates are useful pools of nutrients that can be initially used for exoenzyme production. Once the nutrients and energy are obtained, the microbe's first priority is to preserve homeostasis; maintenance activities include any non-growth activity such as motility, osmoregulation, metabolic pathway shifts, synthesis of DNA/ RNA/enzymes and stress response (Van Bodegom 2007). After these functions are met, the leftover nutrients are allocated to microbial growth to build biomass. When microbes are under nutrient-limited conditions, the leftover element is released as waste through mineralization (if N is in excess) or respiration (if C is in excess). This is termed 'overflow metabolism' and results in elevated mineralization (or respiration) rates that do not accompany an increase in biomass (J. Schimel & Weintraub 2003).

Stoichiometry Rules

Much like human beings, microbes eat a variety of compounds but retain the same stoichiometric composition. Bacterial C:N ratios range from 3:1 to 12:1 and fungal ratios range from 10:1 to 15:1. Regardless of the proportion of bacteria and fungi in the community, overall microbial biomass has a ratio of 4:1 to 8:1 (Horwath 2007; Cleveland & Liptzin 2007). Because of these stoichiometric rules, the C:N and lignin:N ratios can predict decomposition rates- although there are some studies that suggest that nutrient solubility/availability (Rousk & Erland Bååth 2007), microbial community composition and/or resource history of that community can contribute to the rate (Strickland, Osburn, et al. 2009; Strickland, C. Lauber, et al. 2009).

In cross-site studies, different communities have been shown to follow very similar patterns of decomposition when a common substrate is introduced. This suggests that, irrespective of ecosystem and associated microbial community's decomposition capacity, a set of common metabolic pathways stabilizes carbon in the soil long term. The fact that SOM structural, chemical and elemental (C:N:P ratio) properties are generally consistent across ecosystems supports this theory (Horwath 2007). SOM converges on a ratio of 14:1 in less disturbed systems (Cleveland & Liptzin 2007) and

10:1 in cultivated soils (Stevenson 1994). Grandy et al. (2007) studied two environmentally distinct basins in Colorado, and the authors found that, although their uncomplexed carbon fractions were chemically different (presumably from dissimilarities in quality/ quantity of plant inputs and decomposition rates), the SOM chemical compositions were the same. Also, in a preliminary investigation by the current study authors, leachate was collected over time from a compost pile in which cow carcasses were placed. DNA was extracted from the leachate samples and 16S PCR products were submitted for phylogenetic analysis on the 454 pyrosequencing platform. The leachate samples from two different time points contained almost identical ratios of the dominant taxonomic groups, despite the fact that their respective controls were clearly different (Walker et al. 2012).

This evidence supports the theory of microbial biogeography that ‘everything is everywhere, but environment selects’; this elegant phrase, written by Dutch microbiologist Lourens Gerhard Marinus Baas Becking in a 1934 book, describes the theory that all microbial communities contain the same taxa in varying abundances depending on the environmental conditions. The common metabolic pathways and tight microbial biomass C:N range seems to debunk the opposing theory that microbial community structure is a result of stochastic circumstances and dispersal limitations.

Microbial Life Histories

By using established population ecology concepts developed for macrobiota, researchers try to make sense of the complexities of the microbial world. One of the most frequently stolen terms by microbiologists continues to be “r-, K- selection” (Table 1). Developed by MacArthur and Wilson in 1967, these generalized life history strategies continue to be useful to explain population dynamics. K-selected species persist when the habitat is near its carrying capacity (the number of organisms that the area’s resources can support). Therefore, they survive under stable, nutrient limiting conditions, have a slow growth rate and experience a great deal of intra-population competition. In contrast, r-selected species have a high growth efficiency, adapted to a variable environment with plentiful resources (Morris & Blackwood 2007).

There are two other sets of terms that are nearly synonymous with r-, K- strategies that will be valuable to this study. Famous microbiologist Sergei Winogradsky coined the terms autochthonous and zymogenous in 1925 (Table 1). The former is used to describe a stable species that can grow gradually on organic matter with a high substrate affinity. The latter is used to describe a species that proliferates quickly on fresh organic matter. Microbiologists also use the terms copiotroph and oligotroph. Copiotrophs grow quickly in high nutrient environments and are expected to have a fluctuating population size and lower substrate affinities than oligotrophs. In contrast, oligotrophs grow only at low nutrient levels (Killham & Prosser 2007). This slow growth gives oligotrophs an advantage over their counterpart during extended periods of stress, as actively growing organisms are more susceptible to stress (J. P. Schimel et al. 2007). Regardless of naming scheme, an overall theme of two distinct proliferation strategies emerges: one describes a fast-grower in high nutrients level and another is a slow, steady grower in times of stress. It should be noted that these are generalized terms and organisms probably exist on a continuum between the two life histories.

The structures of microbial communities have been shown to change dramatically when fresh detritus is added to the soil (Griffiths et al. 1998). This is evidence that the nutrient level introduces a bias toward certain organisms. The ability of copiotrophs to rapidly utilize new detritus jump-starts the decomposition process. A few studies have even attempted to assign this strategy to individual bacterial taxa. β -Proteobacteria and Bacteroidetes phyla were found to be ecological opportunists and metabolized labile compounds quickly after their placement in the soil (Fierer et al. 2007; P. Padmanabhan et al. 2003).

Table 1. Summary of Life History Strategies

Term	Traits	Reference(s)
Copiotroph	Associated with nutrient- rich environments; adapted to use resources rapidly when available	(Weber 1907; Poindexter 1981)
Oligotroph	Usually found in environments consistently low in nutrients; persist in chronic starvation state	
Zymogenous	Ability to proliferate on fresh organic matter	(Winogradsky 1924)
Autochthonous	Grow steadily on recalcitrant organic matter	
r-selected species	Adapted to variable environment with high levels of resources; high growth efficiency	(MacArthur & E. O. Wilson 1967)
K-selected species	Persist under conditions of scarce resources; stable but slow growth rate	

Bacterial-Fungal Interactions

Although this work focuses more on bacteria's role in the decomposition of organic matter, fungi are no less important in the 'waste management' aspect of an ecosystem. Since they have similar roles, competition for resources is inevitable. Competition between bacteria and fungi can take place in two ways: interference or exploitation. Interference involves one group directly inhibiting the other, possibly using a chemical compound. Exploitation involves one group outcompeting the other for a common resource. Evidence suggests that most bacteria compete via exploitation (Rousk et al. 2008). In addition to competitive pressure, certain abiotic factors affect fungi differently than bacteria. For example, the ratio of fungal to bacterial abundances seems to shift in favor of fungi in acid soils, while bacteria seem to dominate in neutral or slightly basic soils; in general, fungi have a wider pH range than bacteria (Wheeler et al. 1991; Brady & Weil 2008). Both fungi and bacteria respond to temperature similarly

(Allison & Treseder 2008). The correlation between group dominance and elevated CO₂ is unclear (Lipson et al. 2005; Niklaus et al. 2003; Sonnemann & Wolters 2005).

Why Microbial Diversity Matters

The advent of molecular methods has shed some light on the identities of the soil bacteria species and overall community structure. All the organisms of the same species are considered a “population”. All the organisms that live in one area are a “community” and the types and number of species in that community is the “community structure” (Morris & Blackwood 2007). Because of the non-homogenous habitat and fluctuation of environmental conditions, soil communities are very distinct from the communities of other ecosystems, such as oceans, freshwater and human-associated communities (of which, the gut community is relevant in this study). As seen in Figure 5, these two communities are particularly different even at the phylum level of classification (Ley et al. 2008). Soil communities are also more diverse than homogeneous aquatic environments: 4.8×10^9 prokaryotic cells per cm³ of forest soil and 6000 species were

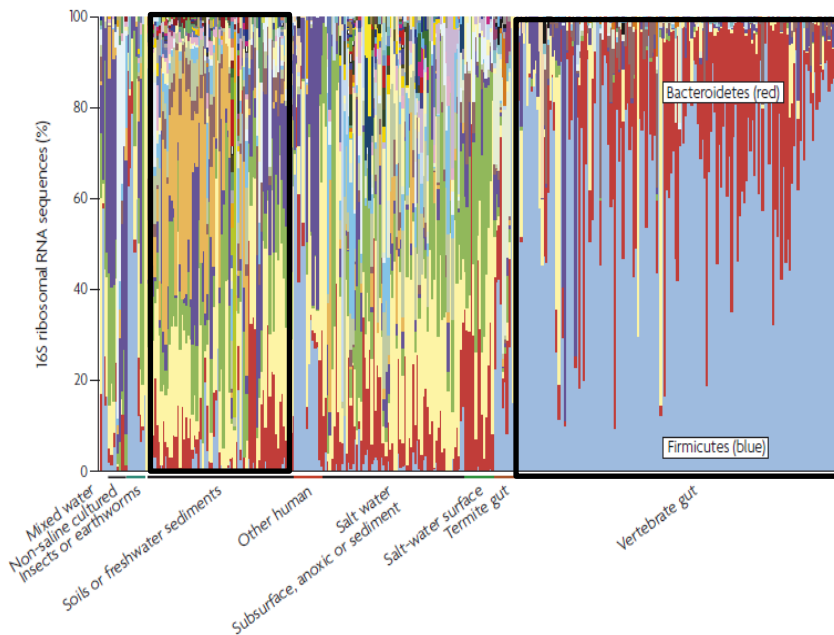


Figure 5. Relative abundances of phyla in 16S rRNA gene libraries from a variety of ecosystems. Boxed in black are soil (left) and gut (right) communities. Figure adapted from Ley et al. (2008).

estimated using fluorescence microscopy and DNA reassociation rates (Torsvik et al. 1998).

As previously discussed, soil microbial communities are similar in their elemental composition and decomposition biochemical pathways. But they are also surprisingly similar in their phenotypic characteristics: just several bacterial phyla dominant most soils- they just vary in relative abundance (Janssen 2006). Top phyla include: Acidobacteria, α -Proteobacteria, β -Proteobacteria, Bacteroidetes, Actinobacteria and Firmicutes. Surprisingly, phylogenetic differences do not equate to changes in decomposition rates, even if those differences are large (Strickland, C. Lauber, et al. 2009; Kemmitt et al. 2008).

Despite unchanged decomposition dynamics, limited study shows phylogenetic differences do change ecosystem process rates (Allison & Martiny 2008). There is much interest in studies that link composition and function but it is difficult when most whole community manipulation only result in a correlated response by the community; although useful for future experimental design, it's not a definitive causation affect (Reed & Martiny 2007). There has been some elucidation of key soil phyla roles in the environment (i.e. nitrification, nitrogen fixation etc.), but general decomposition phyla remain a mystery. Irrespective of the obstacles, understanding the relationship between microbial composition and ecosystem function, like decomposition, is the key to marketing the relevance of microbial community composition in global climate change models- most of which consider microbes irrelevant (Reid 2011). This study aims to investigate the dynamics and roles of microorganisms during decomposition.

Regardless of whether you believe that microbial composition should be included in climate change models, conserving biodiversity in microbial communities is essential. Anthropogenic inputs into the N cycle, pollutants and climate change can affect the microbial world (Zogg et al. 1997; Avrahami et al. 2002). Diversity provides resistance to those environmental changes. It is important to have a variety of organisms that have a slightly different response to a certain biological and physical state. Theoretically, microbial populations can react to stress/disturbances in four ways; they can either withstand change (resistance), return to earlier structure after disturbance (resilience), remain functionally constant but change structure (redundant) or remain a functionally different community indefinitely (Allison & Martiny 2008). Greater diversity increases the probability that the community will be resilient or redundant and maintain the current properties of the ecosystem. In microcosm experiments, there is less variability in ecosystem processes if the community has a greater number of species present (species richness) (Naeem & Li 1997). Species richness, along with species evenness (relative abundance), is a component of species diversity (Chapin et al. 2000).

CHAPTER II OBJECTIVES AND HYPOTHESES

Objective 1

Determine the functional succession of microbial populations in the cadaver decomposition island during decomposition.

Hypothesis 1

Biomass production and respiration will increase rapidly upon introduction of purge fluid and decrease once resources deplete.

Rationale

Copiotrophic bacteria would be expected to proliferate quickly upon the introduction of new labile detritus and remain in the environment while the nutrient levels are high. A sharp escalation in biomass production and respiration should be seen in the Active Decay I stage and remain high until Advanced Decay, as was previously reported (Hopkins et al. 2000; Carter & Tibbett 2008). Once the soil organic carbon depletes and quality of the detritus drops, oligotrophs would increase in relative abundance to the copiotrophs.

Hypothesis 2

There will be a succession of N compounds corresponding to ammonification then nitrification. Subsequent peaks of ammonium and then nitrate/nitrite will occur.

Rationale

As microbes depolymerize proteins and mineralize the amino acids and peptides, the ammonia concentration should increase, and then decline as substrate is used up. This should be followed by an increase in nitrite/nitrate as ammonia oxidation occurs. Other studies recorded a sharp increase in ammonium followed by a decrease (Aitkenhead-Peterson et al. 2012; Vass et al. 1992).

Approach

Ammonium, nitrate/nitrite, phosphate, organic extractable carbon and total nitrogen will be measured. Microbial response patterns, like respiration and leucine incorporation rate, will also be measured.

Objective 2

Determine the taxonomic succession of microbial populations in the CDI during decomposition.

Hypothesis 1

Carcass-associated microbes will enter the soil in the purge fluid and will persist in the soil environment until they are outcompeted by the indigenous soil microbes.

Rationale

During the Bloat stage, destruction of soft tissue is caused by cadaver-associated enteric bacteria. The increased activity of these anaerobes generates high levels of carbon dioxide, methane, and sulfur dioxide, causing the body to bloat. This eventually ruptures the body, sending the enteric bacteria into the soil solution. It is hypothesized that they will colonize their new soil habitat. The abundance of opportunistic indigenous bacteria is hypothesized to rapidly increase soon after the release of bodily fluids (putrefaction). It is hypothesized that the opportunistic bacteria and the cadaver-associated bacteria will co-exist until the CDI becomes nutrient-limited early in the Advanced Decay stage. Then, the cadaver-associated bacteria will be the less competitive community as they are accustomed to a high abundance/diversity, acidic, temperature-stable, nutrient-rich environment (Ley et al. 2008) (Figure 6). In this open soil environment, there is fluctuating temperature, osmotic strength and water content, and oxic conditions (Van Elsas et al. 2011). Although there is no direct evidence to support this theory, the

1967 study by Klein and Casida experimented with different combinations of glucose and ammonium nitrate applied to an artificially inoculated soil of pathogenic *Escherichia coli*. In unamended soils, *E.coli* only lasted 28 days. When glucose was added in levels beyond what is normally found in the soil, *E.coli* only decreased two orders of magnitude, even after 49 days. The addition of ammonium nitrate, regardless of glucose, had no effect on survival. This suggested that the competition for carbon determines enteric bacteria survival.

The bacterial communities found in the gastrointestinal tract and on the skin surface display some interpersonal variability (Fierer, Hamady et al. 2008; Costello, Lauber et al. 2009; Grice, Kong et al. 2009), but every person has the same main phyla, just in different proportions: Actinobacteria, Firmicutes, Bacteroidetes and

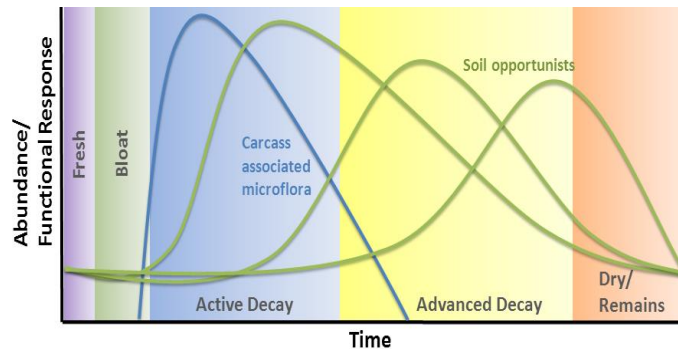


Figure 6. Hypothesized response curves of the two main microbial assemblages in CDI soils: carcass associated microflora (blue) and a succession of soil opportunists (green).

Proteobacteria. Therefore, we should be able to track the gastrointestinal community's fate in the soil regardless of the individual.

Hypothesis 2

The Fungi:Bacteria ratio will increase shortly after the purge fluid enters the soil, then stabilize back to original ratio upon depletion of nutrients.

Rationale

Studies found that the addition of easily available carbon substrates (sugars, amino acids, organic acids, glucose) in very high concentrations favored the increase in fungal growth compared with bacterial growth. At low concentrations, only bacterial growth increased significantly (Griffiths et al. 1999).

Approach

qPCR will be used to quantify human-associated Bacteroides, Fungi (ITS copies), and Bacteria (16S rRNA gene copies).

CHAPTER III MATERIALS AND METHODS

Study Design

Site Description

Founded in 1980 by Dr. William Bass, the University of Tennessee Anthropological Research Facility (ARF) seeks to study human decomposition by conducting research with human cadavers in an outdoor setting (Shirley, Wilson et al. 2011). The 1.3 acre facility is adjacent to the University of Tennessee Medical Center in Knoxville, Tennessee (Figure 7). Soil from this area is classified as a fine, mixed, thermic Typic Paleudalf (more specifically, the Coghill-Corryton Complex series), a well-drained, fine textured clayey soil (NCSS 2004).



Figure 7. Aerial view of UT Anthropological Research Facility (Photo credit: Google Maps)

Climate

Climatic data at the Institute of Agriculture (across the Tennessee River from the ARF) is compiled every 15 minutes by the University of Tennessee Biosystems Engineering and Soil Science (BESS) Department. For the past 8 years, average highs and lows of the area were 21.3 and 10.9 degrees Celsius, respectively; the average humidity was 71.3% and the average yearly rainfall was 124.7 centimeters (Anon 2013)

Study Location Within the ARF

As seen in Figure 8, adapted from Damann (2010), the placement of cadavers at the ARF is non-random due to topography and other access issues. The specific location of each cadaver at ARF has been recorded using GPS; the coordinate data has been layered on the map so the frequency of human decomposition per five by five meter grid unit can be calculated. The units were grouped by the amount of previous decomposition and categorized as none (seen on the figure in white), low (pale yellow), middle (orange), and high decomposition (dark orange) (Damann 2010). It has been suggested that repeated cadaveric inputs might alter microbial populations: the repeated burial of skeletal muscle tissue led to more rapid decomposition tissue mass and more carbon dioxide evolution (Vass et al. 1992; Carter & Tibbett 2008). Every effort was made to obtain plots for the study that, to our knowledge, had not been previously compromised. Placement of the cadavers in this study is marked in red in Figure 8.

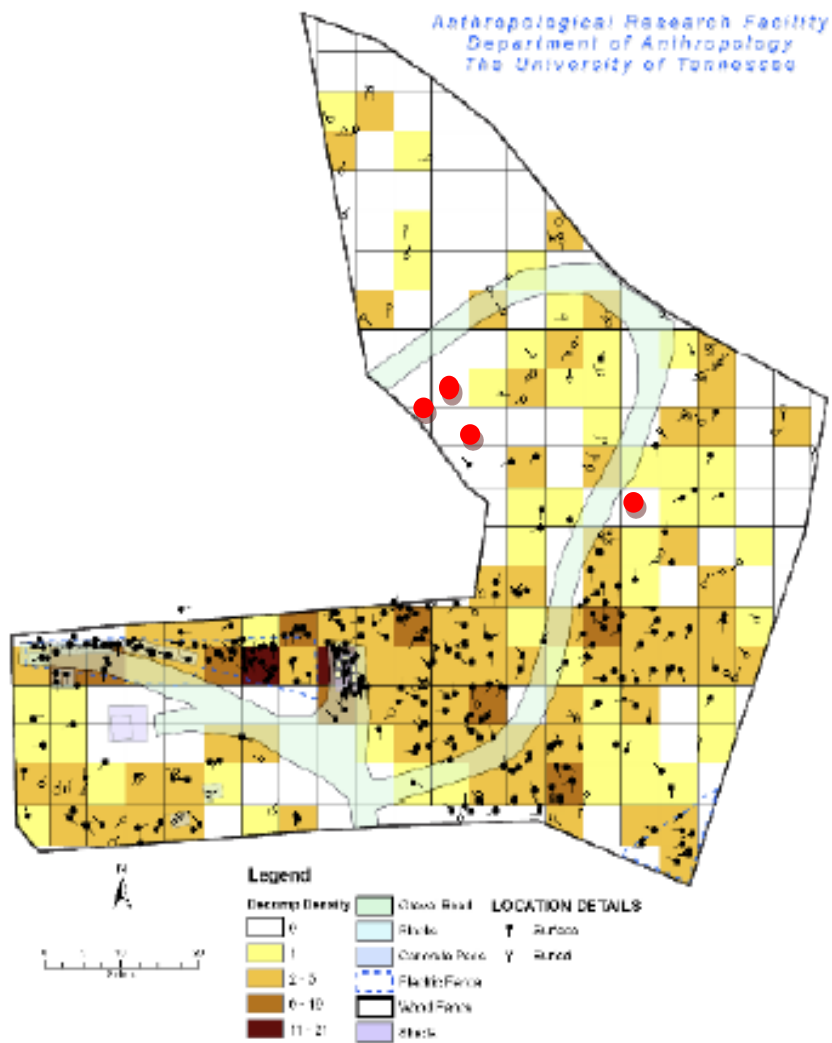


Figure 8. Density of cadaver placement from 2001-2005 at the ARF, Demann (2010). Placement of cadavers from the current study is marked in red.

Soil Sampling

Shortly after death, the cadaver was transported to the William Bass Building, a processing facility for the ARF. It was stored in a refrigerated room until placement. Immediately before placement, the cadaver's cecum was sampled and the incision was re-sealed with standard duct tape. The cecum swabs were transported on ice back to the lab and stored at -20°C until DNA extraction, to be used for a different research project. Before the cadaver was laid on the soil (fresh stage), a baseline soil sample was collected from the future placement site and the control site adjacent to the cadaver (to account for natural seasonal/temporal variation). Using the methodology detailed in Parkinson et al. (2009), an open weave mesh was placed underneath prone cadavers to allow for minimal disturbance while rolling aside for sampling of the soil underneath. At around 10:00 A.M. on the day of sampling, the top 0-3 centimeters of soil beneath the torso was sampled using a 0.34" corer; approximately 20 cores were randomly collected and composited. The frequency of the sampling was determined by the approximate stage of decomposition. Usually, soil was sampled three to four times at the Bloat stage, twice during the Active, and three to five times during the Advanced stage. All composite samples were sieved using standard soil sieve No. 10 (2 mm mesh) and stored at -20°C until DNA extraction. Every attempt was made to remove small rocks, plant material, hair, insects etc. In total, four cadavers (two men and two women) were used in this study (Table 2). Photos were taken each day from different angles to document the decomposition process for data binning purposes, discussed further in the Statistical Analysis section of the Materials and Methods chapter.

Table 2. Metadata associated with cadavers placed in this study

Body Code	Sex	Cause of Death	Approx. weight (pounds)	Date of Placement	Mean temp. through Active Decay (°C)
36-12D	F	natural causes	180	5-21-12	22.4
47-12D	F	UNK	130	6-27-12	27.8
50-12D	M	colon cancer	150	7-6-12	26
67-12D	M	UNK	165	9-19-12	17.2

Normalization for Temperature Differences

Since each cadaver was placed at different times of the year, we needed to account for differences in temperatures during the decomposition process. For the entire length of the study, the hourly temperatures were obtained from the BESS database and used to calculate the Cumulative Degree Hours (CDH) for each cadaver. For greater accuracy, this method uses the twelve hour temperature cycle to describe the temperature's effect on the decomposition process (Vass et al. 2002). The maximum and minimum temperatures from 10:00AM (when sampling usually occurred) to 10:00PM were averaged together and added to the average max/min temperatures of the 10:00PM-10:00AM 12-hour interval to equal the 24-hour interval CDH.

Soil Characteristics

Soil Moisture Content

Soil moisture content was determined gravimetrically by drying 2 grams of each soil sample for approximately a week at 105°C in an Isotemp Oven (Thermo Fisher Scientific, Waltham, MA) to calculate the soil moisture content.

$$\text{Soil Gravimetric Water Content} = \frac{\text{Weight}_{\text{wet soil}} - \text{Weight}_{\text{oven dried soil}}}{\text{Weight}_{\text{oven dried soil}}}$$

Soil Chemistry

First, 8 grams of soil was extracted with 2M KCl by shaking horizontally with the extract at 300RPM and centrifuging 10,000 RPM for 30 minutes at 4°C using a Sorvall[®] RC6 Plus Centrifuge (Thermo Fisher Scientific, Waltham, MA). The supernatant was filtered through 7 centimeter diameter P5 filter paper and stored at -20°C until analysis. The samples were sent to the Biosystems Engineering and Soil Science Water Quality Lab for analysis of nitrogen (Total N, NH₄⁺, NO₂ + NO₃, organic N), total organic carbon and phosphate. A Shimadzu TOC-VCPH analyzer (SHIMADZU Corporation, Kyoto, Japan) was used to determine total carbon by the combustion catalytic oxidation/NDIR method and a Shimadzu N analyzer was used to determine total nitrogen by combustion, then chemiluminescence detection. Nitrate, ammonia, and phosphate were analyzed using a Skalar San⁺⁺ colorimetric autoanalyzer (Skalar Analytical B.V., Breda, The Netherlands). Net N mineralization was calculated as the change in NH₄-N plus (NO₃-NO₂)-N divided by the change in time (in days).

pH

An UltraBasic UB-10 Benchtop Meter (Texas Instrument, Dallas, TX) was calibrated using standard buffers of 4, 7, and 10 prior to use. Soil pore water was extracted by vortexing 5 grams of soil and 10 mL of sterile water for a few minutes. The tube was allowed to sit for a minute to allow settling of soil particles and the electrode was submerged in the pore water until the read-out was constant.

Microbial Activity

Microbial Biomass Production

Microbial biomass production rates was measured using the ^3H - leucine incorporation method (Kirchman 2001) adapted for soil bacteria (E Bååth et al. 2001) Leucine is an amino acid- a building block of protein. When sufficient leucine is added to the medium, *de novo* synthesis is inhibited and radioactively labeled leucine is incorporated into the cell's biomass. Briefly, 0.5 g soil (wet weight) was deposited into a 15 mL conical centrifuge tube. Exactly 10 mL of sterile deionized water was added and shook at 300 RPM for 30 minutes to dislodge soil bacteria. The tubes were centrifuged at 1000 x g for 10 minutes to pellet soil particles. An appropriate volume (700nM) of a 1:10 dilution of tritiated to untritiated ("cold") leucine into 3 microcentrifuge tubes- one "kill" tube for background reading and two "live" sample tubes. Trichloroacetic acid (TCA 100%) was added to the kill tube. Exactly 1.5 mL of soil extract was added to all tubes and they were allowed to incubate for about 1 hour at room temperature. The exact start and stop times were noted. To stop, 100% TCA was added to the live tubes. All tubes were centrifuged in a refrigerated AccuSpin Micro 17R centrifuge (Thermo Fisher Scientific, Waltham, MA) at 13,200 RPM for 10 minutes at 4°C to pellet cells. The supernatant was aspirated off and the pellet was washed with ice cold 5% TCA and centrifuged at 13,200 RPM for 10 minutes at 4°C. The supernatant was aspirated off and the pellet was washed with ice cold 80% ethanol and centrifuged at 13,200 RPM for 10 minutes at 4°C. The supernatant was aspirated and the pellet was allowed to dry overnight. Then, 1 mL of Ecoscint H biodegradable scintillation fluid (National Diagnostics, Atlanta, GA.) was added to the tubes, allowed to sit for 24 hours and counted on a LS 6500 Multi-Purpose Scintillation Counter (Beckman Coulter, Inc. Brea, CA.).

The amount of biomass carbon produced per unit of carbon substrate utilized (in this case leucine) was calculated using an empirical conversion factor estimated for soil bacteria: The conversion factor- 0.54 kilograms of carbon per mole of leucine- was determined by simultaneous measurement of leucine incorporation and bacterial carbon production in ten isolated soil bacterial strains (Michel & Bloem 1993).

Microbial Respiration

Ten grams of soil was added to a 50 mL conical centrifuge tube and was allowed to stand for 24 hours, with the cap vented. Four milliliters of 1.5N NaOH in a 10x75mm disposable borosilicate glass culture tube was inserted into the conical tube as a CO₂ trap. The conical tube was capped and sealed with parafilm and sat undisturbed for approximately 48 hours (exact start and stop times were noted). The vial of NaOH was removed from the tube and solution was transferred to a 15mL falcon tube. 2 milliliters of BaCl₂ was added to each tube and they were centrifuged at 3,500 RPM for 5 minutes in an AccuSpin 3R Centrifuge (Thermo Fisher Scientific, Waltham, MA.) The supernatant was removed to a 50mL disposable beaker. Three drops of phenolphthalein indicator were added to each beaker and it was titrated with 1.0N HCl to a clear endpoint. The amount of HCl (in moles) used to titrate to the endpoint was subtracted from the moles of NaOH originally in the trap to obtain the amount of CO₂ released

Microbial Growth Efficiency

The microbial growth efficiency is the percent of the metabolism that results in biomass, as opposed to mineralization. Because respiration was measured from a microcosm, it includes all microorganisms. The biomass production measurement was derived from leucine incorporation. In short incubation periods, microorganisms with large biomass (i.e. fungi) cannot uptake leucine quickly enough to affect the incorporation rate. Microbial Growth Efficiency (MGE) was estimated by using the following equation:

$$MGE (\%) = \frac{Biomass\ Production}{Biomass\ Production + Respiration} * 100$$

DNA Extraction and Preparation

DNA Extraction

All samples were extracted using the PowerLyzer™ PowerSoil® DNA Isolation Kit (MOBIO Laboratories, Inc. Carlsbad, CA.), with three key protocol changes. In brief, 0.25 grams of soil was weighed into a PowerLyzer™ Glass Bead Tube, 0.1mm. The “bead solution” was added and the tubes were incubated at 65°C for 10 minutes in a Precision® 182 Water Bath (Thermo Fisher Scientific, Waltham, MA.). The tubes were temporarily vented and incubated at 95°C in an Isotemp® heat block (Thermo Fisher Scientific, Waltham, MA.) for another 10 minutes. These two steps were not included in the original kit protocol, but previous optimization resulted in higher quality yields with these changes. The SDS solution (“Solution 1”) was added as normal and the tubes were placed into the PowerLyzer™ 24 (MOBIO Laboratories, Inc. Carlsbad, CA.). The sample ran for 45 seconds at 3,100 RPM. They were then centrifuge at 10,000 x g for 30 seconds at room temperature in an AccuSpin Micro 17R centrifuge (Thermo Fisher Scientific, Waltham, MA). The supernatant was transferred to a clean tube and a patented Inhibitor Removal Technology® (IRT) solution was added. The tubes were incubated on ice for 5 minutes. The tubes were then centrifuged, and the supernatant was treated to another round of IRT solution (“Solution 3”) to precipitate additional organic and inorganic material like humic acid, cellular debris etc. After incubation on ice for 5 minutes, the samples were centrifuged for 2 minutes (protocol change, originally: 1 minute). A high concentration salt solution (“Solution 4”) was added to the removed supernatant and the mixture was loaded onto a Spin Filter. The Spin Filters were centrifuged at 10,000 x g for 1 minute and the flow-through was discarded. This was repeated in batches until no more sample remained. All of the DNA should be bound to the silica membrane of the Spin Filter. An ethanol wash (“Solution 5”) was added to remove any extra salts, humic acid and other contaminants, and centrifuged for 30 seconds at 10,000 x g. The flow-through was discarded and the tubes were centrifuged again at the same conditions to ensure all traces of the ethanol wash were gone. The spin

filter was then placed in a clean tube and eluted with nuclease-free water (Thermo Fisher Scientific Inc. Waltham, MA.). Extracted DNA was stored at -20°C.

DNA Quantification

The DNA concentration of each sample was measured using the fluorometry-based Quant-it™ PicoGreen® dsDNA kit (Invitrogen, Eugene, OR). To quickly summarize the protocol, a standard curve was made using λ Standard DNA (Invitrogen, Eugene, OR) by diluting to the concentrations: 100, 50, 25, 12.5, 6.25, 3.13, 1.56, and 0 ng per well. DNA extractions were diluted 1:10 to fall within this curve. The standards were added to a black 96-well plate in duplicates. 1X TE buffer and sample was added to the sample wells. Then, working solution of Quant-iT™ PicoGreen® reagent was mixed into each sample and incubated in the dark for 2 to 5 minutes at room temperature. After incubation, the fluorescence was measured using a Synergy HT microplate reader (BioTek, Winooski, VT) at the following wavelengths: excitation 480 nm, emission 520 nm. The fluorescence value of the 0 ng per well (no DNA control) was subtracted from the sample value and the standard curve was used to calculate DNA concentrations.

Quantitative PCR (qPCR)

Creation of Bacterial 16S Plasmid for qPCR Standard

The 16S rRNA gene was amplified from genomic DNA of *Alphaproteobacteria sphingomonas*, previously isolated from soil at the Kellogg Biological Station (Kalamazoo, MI.), using the universal bacterial primers 8F and 1492R (Hicks et al. 1992). For each 25 μ l PCR reaction, 12.5 μ l Finnzymes Phusion High Fidelity PCR Master Mix (Thermo Fisher Scientific Inc. Waltham, MA.), 9.5 μ l of nuclease-free water (Thermo Fisher Scientific Inc. Waltham, MA.), 1.0 μ l of 8F primer (10 μ M) and 1.0 μ l of 1492R primer (10 μ M) (Eurofins MWG Operon, Huntsville, AL.) and 1.0 μ l template DNA were added together. PCR was performed on a Mastercycler® pro Thermocycler (Eppendorf, Hauppauge, NY.) using the following protocol: 95°C for 5 minutes, then 40 cycles of denaturing at 95°C for 30 seconds, annealing at 45°C for 30 seconds, and extending at 72°C for 30 seconds, with 10 minutes at 72°C for final extension. To confirm the success of the PCR reaction, gel electrophoresis (1.5% (w/v) agarose gel with Ethidium Bromide) was used.

The rest of the protocol follows the pGEM®-T Vector System (Promega Corporation, Madison, WI.). Briefly, a ligation reaction combines 2X Rapid Ligation Buffer, T4 DNA Ligase, pGEM®-T Vector, and PCR product. This reaction was allowed to incubate overnight at 4°C. An aliquot of ligation reaction was added to a 15 mL falcon tube on ice. Thawed, mixed JM109 High Efficiency Competent Cells (Promega Corporation, Madison, WI.) were added to the tube and placed on ice for 20 minutes. Then, the cells were heat-shocked in a 42°C water bath for 45 seconds. The tube was returned to the ice for 2 minutes. Room temperature SOC medium was added to the transformed cells and incubated for 1.5 hours at 37°C, shaking at 150 RPM. The cells were plated on LB/ampicillin/IPTG/X-Gal plates and incubated overnight at 37°C. Afterward, the plates were stored overnight in 4°C to amplify the blue color in the

colonies. A white colony was then picked from the plate and inoculated to liquid LB/ampicillin broth.

Once the cells reached an appropriate growth density, they were harvested for plasmid isolation using the Wizard[®] Plus SV Miniprep DNA Purification System (Promega Corporation, Madison, WI.). In summary, the cells were centrifuged for 5 minutes at 10,000 x g in an AccuSpin Micro 17R centrifuge (Thermo Fisher Scientific, Waltham, MA). The supernatant was poured off and the pellet suspended in Cell Resuspension Solution. Cell Lysis Solution was added, mixed and allowed to incubate until a partial clearing was seen in the lysate. Alkaline Protease Solution was added, mixed and allowed to incubate for 5 minutes to inactivate proteins such as endonucleases that were released during cell lysis. A Neutralization Solution was added, the tube mixed and then centrifuged at 14,000 x g for 10 minutes at room temperature. The cleared lysate was transferred to a Spin Column and centrifuged at 14,000 x g for 1 minute. The flow-through was discarded and Column Wash solution was added to the Spin Column. After centrifugation at 14,000 x g for 1 minute, the flow-through was discarded and the wash/centrifuge/decant step was repeated. The Spin Column was centrifuged again to remove any residual Column Wash for 2 minutes at 14,000 x g and transferred to a clean tube for elution into nuclease-free water (Thermo Fisher Scientific Inc. Waltham, MA.). The plasmid was stored long-term at -20°C. To confirm the presence of the insert in the plasmid, the plasmid was sequenced at the University of Tennessee Knoxville Molecular Biology Resource Facility on a 3730 DNA Analyzer (Applied Biosystems, Foster City, CA.) using the T7 primer set.

Quantification of Bacterial 16S rRNA genes

To enumerate copies of bacterial 16S rRNA genes, universal bacterial primers 1055F and 1392R were used in qPCR (G J Olsen, et al. 2003). For each 25µl qPCR reaction, 12.5µl Maxima[®] SYBR Green/Fluorescein qPCR Master Mix (2X) (Thermo Fisher Scientific Inc. Waltham, MA.), 5.5µl of nuclease-free water (Thermo Fisher Scientific Inc. Waltham, MA.), 1.0µl of 1055F primer (10 µM) and 1.0µl of 1392R primer (10 µM) (Eurofins MWG Operon, Huntsville, AL.) and 5.0µl template DNA were added together. The standard curve was made by diluting the plasmid previously mentioned from 10⁸ to 10⁴ copies per reaction. The DNA extraction of each sample was diluted 100-fold to fall within this standard curve and the reactions were done in triplicates. qPCR was performed on a C1000 Thermal Cycler with a CFX96 Real Time System (Bio-Rad, Hercules, CA.) using the following protocol: 95°C for 10 minutes (hot start), then 40 cycles of denaturing at 95°C for 30 seconds, annealing at 51°C for 25 seconds, and extending at 72°C for 25 seconds. Gene copy numbers were found using an equation for the regression line that related the cycle threshold (C(t)) value to the known number of copies in the standards.

Quantification of Human-Associated Bacteriodes

The gastrointestinal flora of humans has recently been elucidated (Costello et al. 2009) and this unique community can be tracked as it enters the soil by the real-time PCR assay. We will focus on enumerating human-associated *Bacteriodes* (HuBac) throughout the decomposition process following the method of Layton et al. (2006).

HuBac primers, HuBac566f and HuBac692r, were designed from partial alignments of *Bacteroides* 16S genes from fecal source libraries and GenBank (Layton et al. 2006). For each 25 µl qPCR reaction, 12.5 µl Absolute Blue qPCR Master Mix (Thermo Fisher Scientific Inc. Waltham, MA.), 6.5 µl of nuclease-free water (Thermo Fisher Scientific Inc. Waltham, MA.), 1.5 µl of HuBac566f primer (10 µM), 1.0 µl of HuBac692r primer (10 µM) and 0.5 µl HuBac594Bhqf probe (10 µM) (Eurofins MWG Operon, Huntsville, AL.) and 2.5 µl template DNA were added together. All qPCR reactions were performed in triplicate. The standard curve ranged from 10^1 to 10^7 copies per reaction. The plasmid used for the standard curve was obtained from the A. Layton lab group (UTK). qPCR was performed on a C1000 Thermal Cycler with a CFX96 Real Time System (Bio-Rad, Hercules, CA.) using the following protocol: 50°C for 2 minutes, 95°C for 15 minutes (hot start), then 40 cycles of denaturing at 95°C for 30 seconds, annealing at 60°C for 45 seconds. Gene copy numbers were found using an equation for the regression line that related the cycle threshold (C(t)) value to the known number of copies in the standards.

Quantification of Fungal ITS Region

To determine shifts in bacterial and fungal populations during decomposition, a DNA-based approach known as quantitative PCR (qPCR) will be used, following the method of (Fierer et al. 2005). Oligonucleotides specific to bacterial 16S rRNA and fungal ITS region (primers) will amplify DNA and a fluorescent reporter molecule will bind to the new double-stranded DNA and the amount of fluorescence is measured to determine the abundance of gene copies. Since fungi have a variable number of nuclei and bacteria can have more than one 16S rRNA gene copies, it cannot be used to determine absolute cell abundances (Klappenbach et al. 2000). Also, DNA extraction and PCR amplification introduce their own bias: extraction efficiencies may differ; primers may not target genes consistently in all taxa (Martin-Laurent et al. 2001). Despite these disadvantages, we can perform relative comparisons between samples in this study and study how the ratios change during decomposition.

To create the plasmid for the qPCR standard curve, the Fungal ITS I region was amplified from genomic DNA of *Bipolaris oryzae* organism, obtained from the B. Ownley lab group (UTK), using the ITS1f and 5.8S-R primers (Gardes & Bruns 1993; R Vilgalys & Hester 1990). For each 25 µl PCR reaction, 12.5 µl Finnzymes Phusion High Fidelity PCR Master Mix (Thermo Fisher Scientific Inc. Waltham, MA.), 9.5 µl of nuclease-free water (Thermo Fisher Scientific Inc. Waltham, MA.), 1.0 µl of ITS1f primer (10 µM) and 1.0 µl of 5.8S-R primer (10 µM) (Eurofins MWG Operon, Huntsville, AL.) and 1.0 µl template DNA were added together. PCR was performed on a Mastercycler[®] pro Thermocycler (Eppendorf, Hauppauge, NY.) using the following protocol: 95°C for 5 minutes, then 40 cycles of denaturing at 95°C for 1 minute, annealing at 53°C for 30 seconds, and extending at 72°C for 1 minute, with a final extension at 72°C for 10 minutes. To confirm the success of the PCR reaction, gel electrophoresis (1.5% (w/v) agarose gel with Ethidium Bromide) was used. The rest of the protocol for ligation, transformation and harvesting were identical to the 16S rRNA gene plasmid creation protocol previously discussed.

For each 25 μl qPCR reaction, 12.5 μl Maxima[®] SYBR Green/Fluorescein qPCR Master Mix (2X) (Thermo Fisher Scientific Inc. Waltham, MA.), 5.5 μl of nuclease-free water (Thermo Fisher Scientific Inc. Waltham, MA.), 1.0 μl of ITS1f primer (10 μM) and 1.0 μl of 5.8s primer (10 μM) (Eurofins MWG Operon, Huntsville, AL.) and 5.0 μl template DNA were added together. The standard curve was made by diluting the plasmid previously mentioned from 10^8 to 10^3 copies per reaction. qPCR was performed on a C1000 Thermal Cycler with a CFX96 Real Time System (Bio-Rad, Hercules, CA.) using the following protocol: 95°C for 15 minutes, then 40 cycles of denaturing at 95°C for 1 minute, annealing at 53°C for 30 seconds, and extending at 72°C for 1 minute (Fierer et al. 2005). Gene copy numbers were found using an equation for the regression line that related the cycle threshold (C(t)) value to the known number of copies in the standards. The fungal ITS copy number was divided by the total bacterial 16S rRNA gene copy number from the same sample.

Statistical Analysis

Where appropriate, data were standardized to grams of dry weight soil. Surprisingly, the moisture content in the CDI did not significantly differ from the control soils (Wilcoxon Signed Rank Test, data not shown).

Binning

Upon the conclusion of the study, images taken of the cadavers throughout the decomposition process were reviewed to determine the traditional decomposition stage as categorized by J.A. Payne (Payne 1965). Since the cadavers decomposed at different temperatures, the rates of decomposition varied. In order to combine the four cadavers as experimental replicates, data from each cadaver were binned by decomposition stage during which they were obtained. To attain a higher resolution of data visualization, intermediate stages were added. The data was divided into the following stages for each cadaver: Initial (before placement of cadaver), Bloat, Bloat-Active, Active, Initial Advanced Decay, Advanced Decay I, Advanced Decay II, Advanced Decay III. Their abbreviations for the remainder of the paper: Initial, Bloat, Bloat-Act, Act, Initial Adv, Adv I, Adv II, Adv III, respectively. Then, data from each stage for replicate cadavers were combined and subjected to graphical and statistical analysis.

Statistical Tests

Spearman rank-order correlation (r_s) was used to estimate the association between paired samples. This rank-based measure of association was used because the data was not expected to follow a normal distribution. Asymptotic t approximation was used to test the association value as zero. Select correlations were graphed with the ggplot2 package of the open source software, R (Wickham 2009; R Core Team 2012). Non-parametric alternatives to Student's t test, Wilcoxon signed rank and Wilcoxon rank sum tests, were used to determine if the CDI samples in each decomposition stage were significantly different from the control samples at the 5% level. A Wilcoxon signed rank test assesses the null hypothesis that the median difference between pairs of observations

was zero. When Wilcoxon rank sum test (also known as the Mann-Whitney test) was carried out in unpaired cases, the null hypothesis was that the population medians are equal. All statistical tests were performed in R (R Core Team 2012).

CHAPTER IV RESULTS

Four cadavers were placed at the University of Tennessee Anthropological Research Facility (ARF) on plots that, to the best of our knowledge, had not been previously used for decomposition studies. The study was conducted through the summer and fall of 2012 when the average temperatures were 22.4, 27.8, 26.0, and 17.2 degrees Celsius for cadavers #36, #47, #50, and #67 respectively. An open weave mesh was placed underneath the cadavers to allow for minimal disturbance while rolling aside for sampling of the top 0-3 centimeters of soil beneath the torso. Usually, soil was sampled three to four times at the Bloat stage, twice during the Active, and three to five times during the Advanced stage. The study length did not allow for sampling during the Dry/Remains stage. Cadavers #36, #47, #50 and #67 were sampled for 87, 198, 83 and 114 days, respectively. For each composite soil sample, the soil solution was extracted and soil chemistry, pH, soil moisture and microbial activity were measured. Also, human-associated *Bacteroides*, total bacterial, and total fungal abundances were measured via qPCR. Data from each cadaver were binned by decomposition stage during which they were obtained. The categorization of the sampling days can be found in Appendix, Table A1.

Bacterial biomass production rates

During the Active Decay stage of all cadavers, a sharp decrease in ³H-leucine incorporation rate was seen in the cadaver decomposition island (CDI) soils compared to controls; however, because of the variability between cadavers, the average bacterial production rate in CDI soils was not significantly different than the control at any stage (Table 3). All CDI soils in Advanced Decay stage, except for #47, increased in leucine incorporation rates under the cadavers to surpass the control soil rates (Figure 9). Leucine incorporation rates were significantly correlated to extractable organic carbon, pH (Table 4) and total 16S rRNA gene copies (Figure 10).

Table 3. Summary of mean and standard deviations from all CDI data. Asterisk (*) indicates value was significantly above respective control value using the Wilcoxon Signed Rank Test (p<0.05). A double asterisk () indicates value was significantly above initial value using the Wilcoxon Rank Sum test (p<0.05)**

Variable	Decomposition Stage							
	Initial	Bloat	Bloat-Active	Active	Initial Advanced	Advanced I	Advanced II	Advanced III
pH	6.678 ±0.151	6.243 ±1.054	7.025 ±1.126	6.622 ±0.978	6.628 ±0.935	7.163 ±1.061	7.203 ±0.906	6.023 ±0.380
Dry weight (%)	0.785 ±0.106	0.789 ±0.088	0.761 ±0.042	0.742 ±0.091	0.744 ±0.028	0.712 ±0.053	0.710 ±0.106	0.696 ±0.143
Total 16S gene copies (log/gdw)	10.295 ±0.716	10.225 ±0.771	10.681 ±0.731*	10.255 ±0.858	10.269 ±0.836	10.696 ±0.728	10.695 ±0.233	11.169 ±NA
HuBac 16S gene copies (log/gdw)	1.367 ±2.734	3.306 ±3.652	6.958 ±2.862**	7.691 ±0.768**	7.567 ±0.490**	7.565 ±0.962**	7.866 ±1.287**	7.347 ±1.352**
Fungi ITS gene copies (log/gdw)	9.179 ±0.524	9.143 ±0.517	9.444 ±0.444	9.749 ±0.324	9.706 ±0.478	9.740 ±0.591	9.574 ±0.620	9.468 ±0.354
EOC (mg C/gdw)	0.310 ±0.245	0.623 ±0.397*	1.889 ±0.337*	5.565 ±2.831*	5.989 ±1.932*	5.998 ±1.800*	5.901 ±3.175*	4.301 ±5.149
PO4 (ppm)	0.294 ±0.215	1.237 ±1.334	1.04 ±1.059	1.412 ±1.422	2.058 ±1.582	2.860 ±2.154	5.177 ±5.736*	0.704 ±0.316
NO₃-NO₂ (mg N/gdw)	0.021 ±0.017	0.132 ±0.241	0.102 ±0.162*	0.067 ±0.098	0.039 ±0.075	0.041 ±0.043	0.208 ±0.238	0.045 ±0.054
NH₃ (mg N/gdw)	0.011 ±0.008	0.129 ±0.117*	1.189 ±0.845*	2.541 ±2.103*	2.695 ±0.812*	3.762 ±1.702*	3.097 ±0.870*	0.710 ±0.933
TN (mg/gdw)	0.046 ±0.023	0.371 ±0.335*	1.779 ±1.256	3.244 ±2.036*	3.182 ±0.610*	4.482 ±1.197	3.739 ±0.970*	1.300 ±1.589
Net Mineralization (mg N/gdw/day)	NA	0.106 ±0.166	0.231 ±0.246*	0.362 ±0.320*	0.062 ±0.364	-0.070 ±0.276	-0.010 ±0.042	-0.030 ±0.005
Leucine Incorporation (μmol Leu/day/gdw)	1.01E-03 ±5.52E-04	1.24E-03 ±9.96E-04	1.86E-03 ±1.72E-03	3.66E-04 ±4.75E-04	2.63E-04 ±4.90E-04	6.42E-04 ±9.29E-04	5.05E-04 ±4.08E-04	1.15E-03 ±9.87E-04
Respiration (mg C/hr/gdw)	3.22E-03 ±1.47E-03	9.07E-03 ±6.30E-03	2.48E-02 ±8.44E-03*	3.16E-02 ±1.12E-02*	2.07E-02 ±4.39E-03	3.74E-02 ±1.12E-02*	3.03E-02 ±1.09E-02*	2.42E-02 ±1.54E-02
Microbial Growth Efficiency (%)	0.576 ±0.344	0.206 ±0.160	0.170 ±0.160*	0.021 ±0.037*	0.023 ±0.041	0.034 ±0.050	0.039 ±0.037	0.241 ±0.340

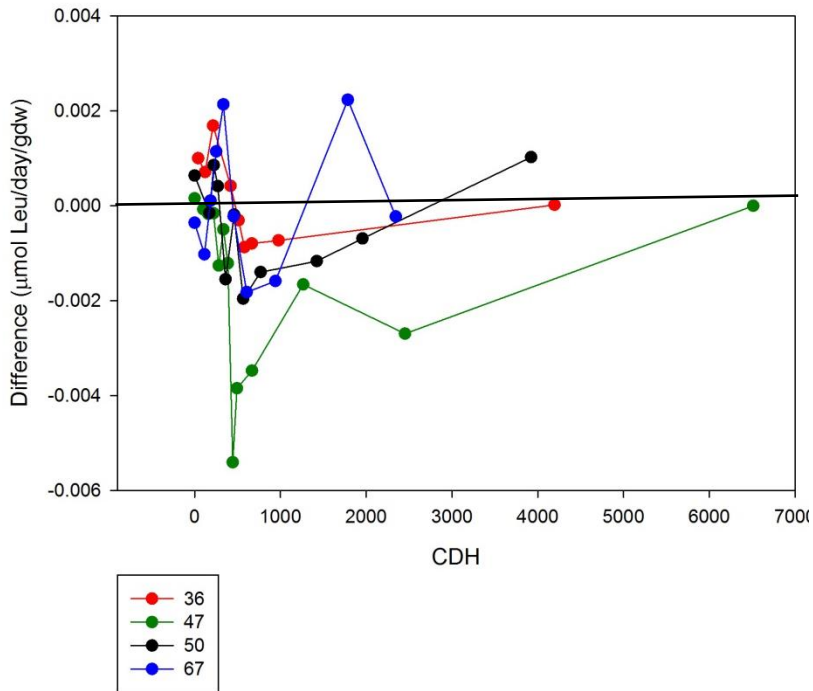


Figure 9. Difference in bacterial biomass production between cadaver decomposition island (CDI) soils for four cadavers (36, 47, 50, 67) and control soils, estimated from leucine incorporation rates in bacterial suspensions extracted from soil. Data is presented by cumulative degree hours (CDH).

Table 4. Variables that were significantly correlated with Spearman Rank-Order Correlation coefficients, (r_s) > 0.50.

Variable 1	Variable 2	N	r_s	p-value
NH ₃	Total Extractable Nitrogen	47	0.9500	0
Total Extractable Nitrogen	Extractable Organic Carbon	47	0.8533	0
Total 16S gene copies	Leucine Incorporation Rate	38	0.8225	3.87E-08
NH ₃	Extractable Organic Carbon	47	0.7750	0
pH	Leucine Incorporation Rate	44	0.7047	9.37E-08
Respiration	NH ₃	45	0.6628	1.48E-06
Respiration	Total Extractable Nitrogen	45	0.6390	4.10E-06
Respiration	Extractable Organic Carbon	45	0.5847	3.50E-05
PO ₄	Extractable Organic Carbon	37	0.5116	0.00140
pH	Microbial Growth Efficiency	42	0.5092	5.73E-04
Extractable Organic Carbon	Leucine Incorporation Rate	44	-0.5248	2.55E-04
Microbial Growth Efficiency	Total Extractable Nitrogen	42	-0.6098	2.70E-05
Microbial Growth Efficiency	Extractable Organic Carbon	42	-0.7757	4.14E-08

Microbial Respiration

The microbial respiration rate remained relatively constant in all of the control soils over the course of the study with bin averages ranging from 0.004-0.009 mg C/hr/gdw (data not shown). In all of the CDI soils, while the cadavers were in Bloat stage, there was a small increase in respiration (Figure 11). Then, two significant increases in respiration were seen (Table 3). The first increase occurred during the Active Decay stage for each cadaver (best seen in Figure 12). The second increase occurred near the beginning of Advanced Decay stage. Respiration was significantly correlated with total extractable organic carbon (Figure 13), total extractable nitrogen (Figure 13), and extractable organic carbon (Table 4).

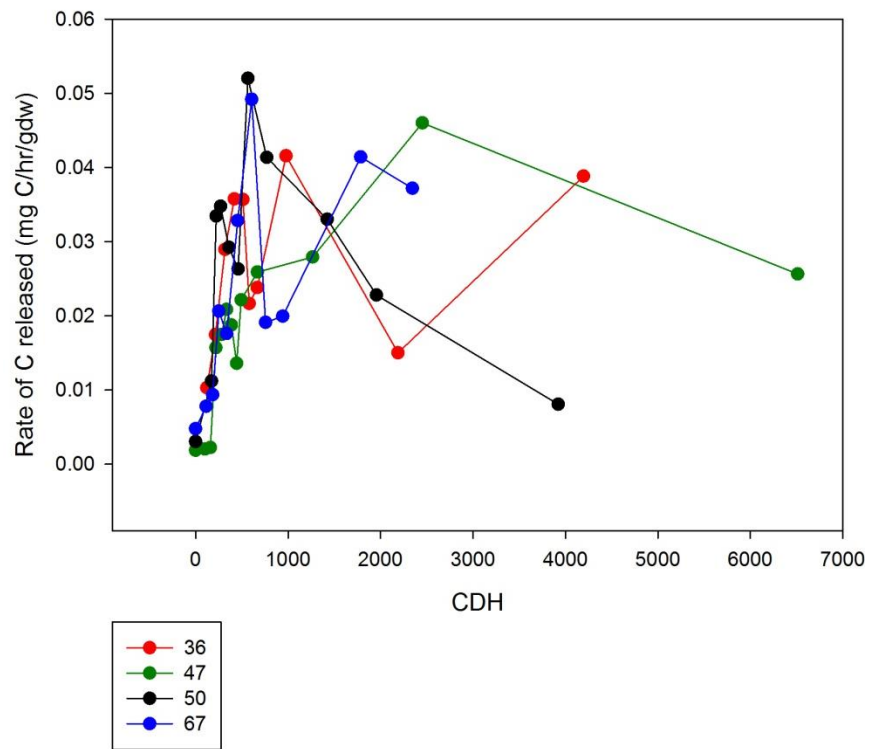


Figure 11. Soil respiration rates during a 48 hour incubation at room temperature (mg CO₂-C per hour per gram dry weight (gdw)) as a function of the cumulative degree hours (CDH) in soils beneath cadavers and their respective control samples.

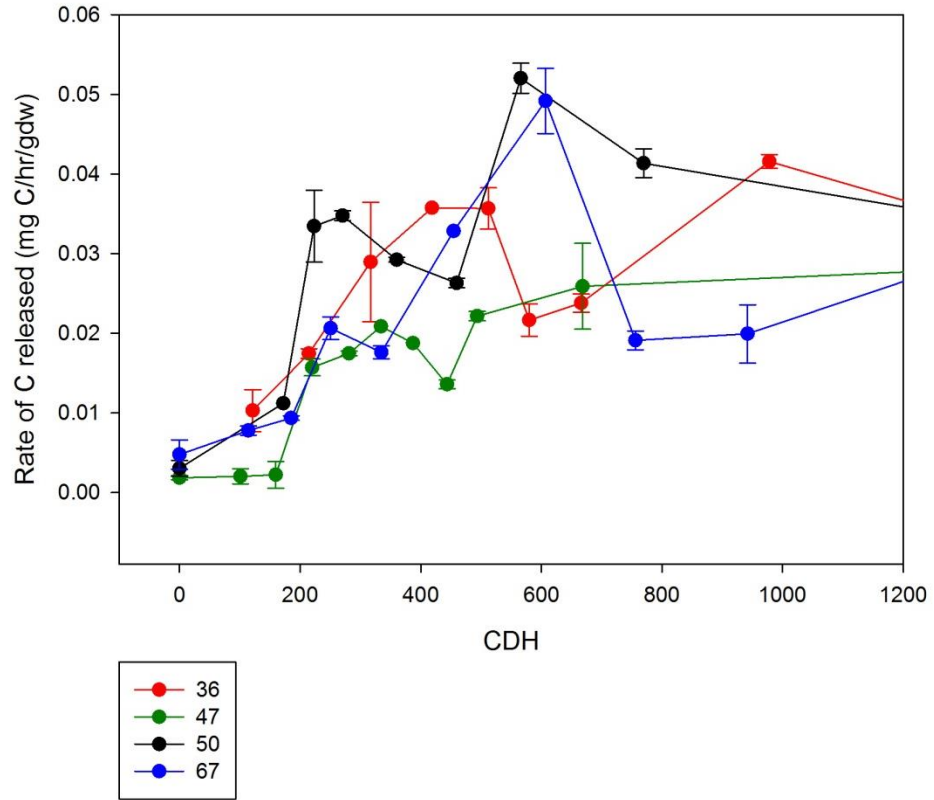


Figure 12. Data presented in Figure 11 is here shown for just the Bloat and Active Decay stages. Data is presented by cumulative degree hours (CDH).

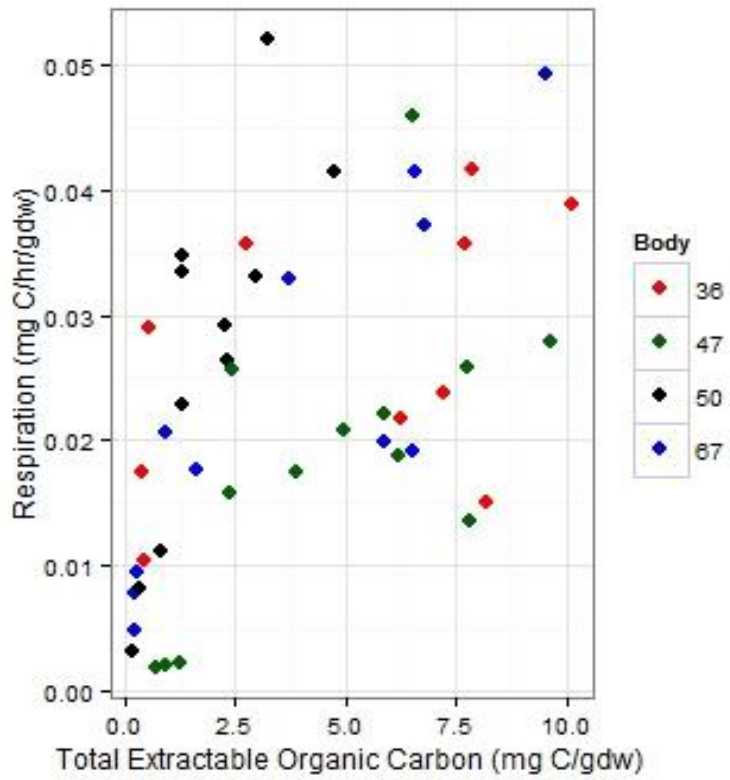


Figure 13. Correlation between total extractable organic carbon and microbial respiration ($r_s=0.5847$, $p<0.001$).

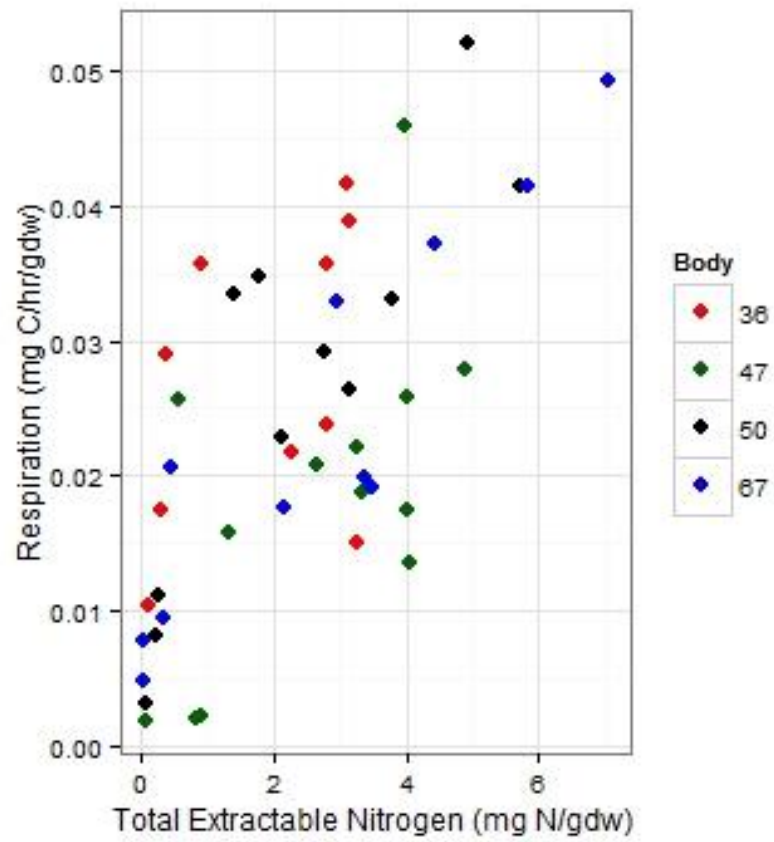


Figure 14. Correlation between total extractable nitrogen and microbial respiration ($r_s=0.6390$, $p<0.001$).

Microbial Growth Efficiency

While the control soils are characterized by considerable variability in the microbial growth efficiency (MGE), the main trend in CDI soils was the steady decrease of MGE throughout the decomposition process until the Advanced Decay III stage, where it returned to fifty percent of the initial value (Figure 15). MGE was significantly lower than control soils during the Bloat and Bloat-Active transition (Table 3). Microbial growth efficiency was significantly inversely correlated to pH, total extractable nitrogen, and extractable organic carbon (Table 4).

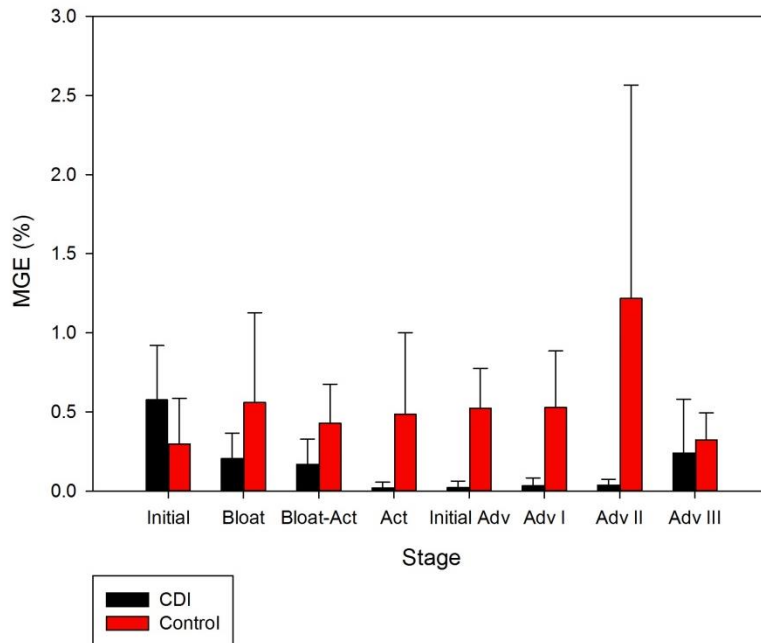


Figure 15. Microbial growth efficiency, calculated as biomass production rate divided by the sum of biomass production rate and respiration rate, during the different stages of decomposition. Abbreviation key as follows: Bloat-Act (Bloat-Active), Act (Active), Initial Adv (Initial Advanced Decay), Adv I (Advanced Decay I), Adv II (Advanced Decay II), Adv III (Advanced Decay III).

Nitrogen Fractions

In the control soils, the concentration of total extractable nitrogen (TN) was variable, ranging from 0.01 to 0.8 mg N/gdw with nitrate/nitrite and ammonium alternating as main contributors to the TN pool during the duration of the study (Figure 16). The TN in CDI soils was up to 140 times greater than the control soils. The most obvious trend in the CDI soils was strong correlation between ammonium and TN (Table 4). Nitrate/nitrite-N was only significant in the Bloat-Active Decay stage. At the start of the Bloat stage, in the CDI soils, there was a significant increase in ammonium- which drove the TN concentration higher as well. Another common observation worth noting: at the end of Active Decay stage, underneath all of the cadavers except for #50, there was a drop in TN/ammonium-N followed by an increase back to previous concentrations. The high variability in Advanced Decay III stage can be accounted for by the fact that TN and ammonium concentrations vary depending on the cadaver: soils beneath #47 and #50 returned to original levels while the soils beneath #36 and #67 remained high.

TN in the CDIs was significant in the Bloat, Active, Initial Advanced and Advanced Decay II stages, while ammonia-N was significant from Bloat to Advanced Decay II stages (Table 3). Ammonia and TN were significantly correlated to extractable organic carbon, respiration and only TN was significantly inversely correlated to microbial growth efficiency (Table 4).

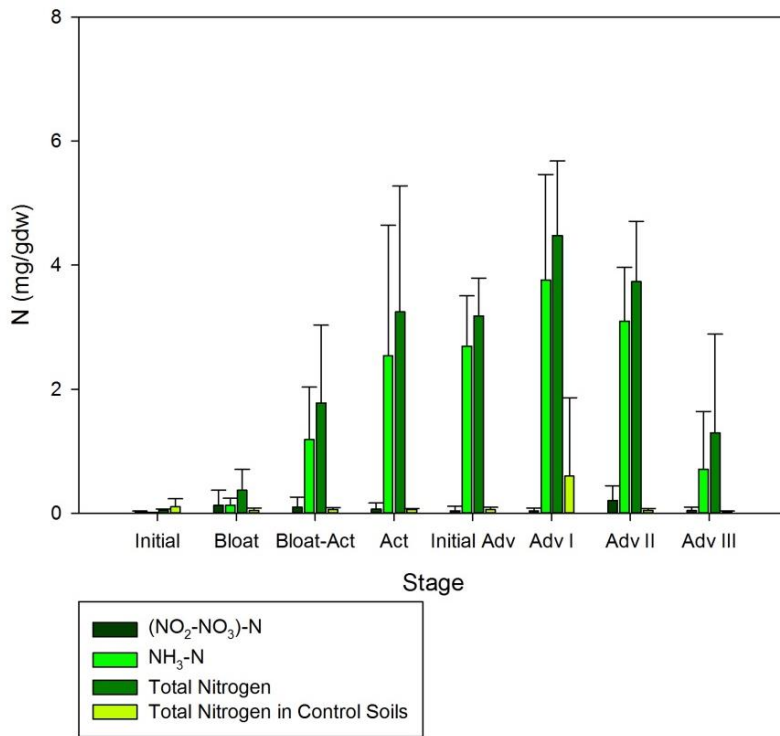


Figure 16. Extractable Nitrogen fractions of cadaver decomposition island (CDI) soils during decomposition compared to total nitrogen concentrations in the control soils. Abbreviation key as follows: Bloat-Act (Bloat-Active), Act (Active), Initial Adv (Initial Advanced Decay), Adv I (Advanced Decay I), Adv II (Advanced Decay II), Adv III (Advanced Decay III).

Net Nitrogen Mineralization

Net N mineralization was calculated as the change in $\text{NH}_4\text{-N}$ plus $(\text{NO}_3\text{-NO}_2)\text{-N}$ divided by the change in time (in days). Regardless of the net nitrogen mineralization behavior in the control soils, the most obvious trend in the CDI soils was the sharp increase at around 500 CDH (Figure 19). As a whole, the net N mineralization increased significantly in the Bloat and Bloat-Active stages (Table 3). In every CDI, except #50, the peak corresponded to the entire Active Decay stage and the first peak in respiration; in #50, the increase in net N mineralization slightly preceded the increase in respiration.

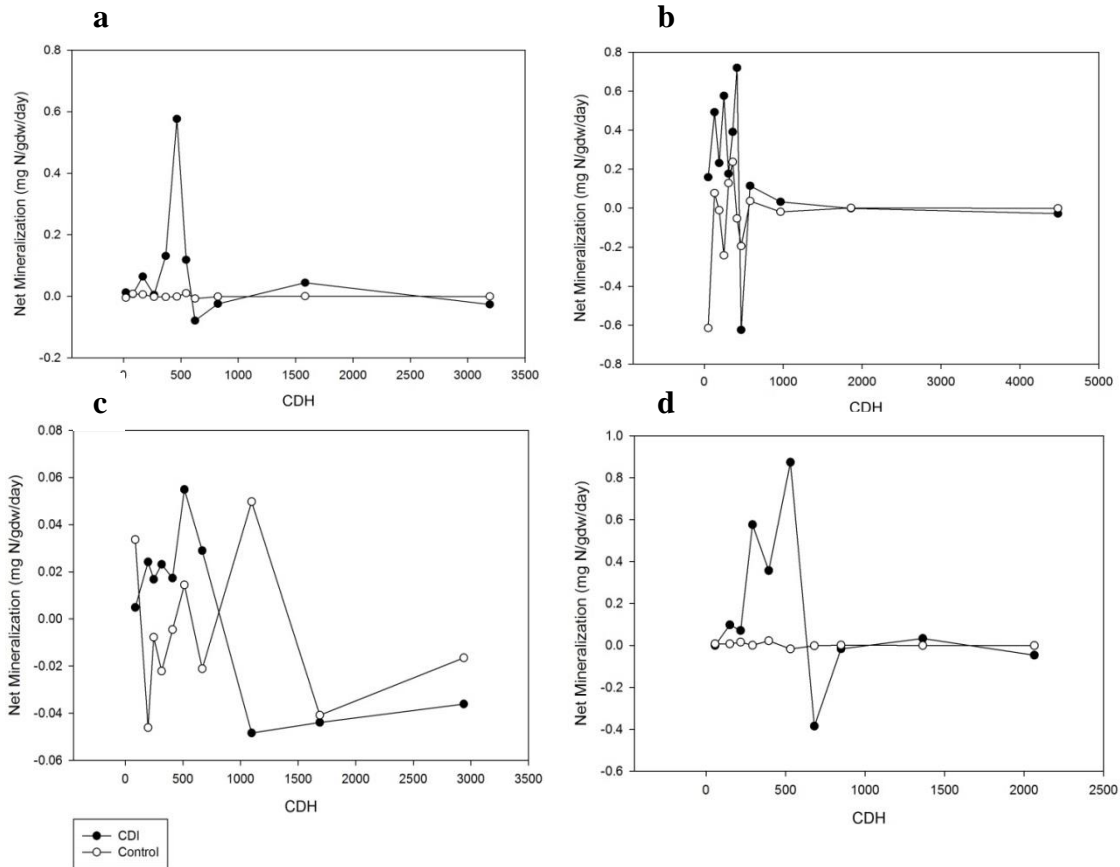


Figure 17. Net N mineralization in cadaver decomposition island (CDI) soils and their respective control soils (a) #36, (b) #47, (c) #50, and (d) #67. Data is presented by cumulative degree hours (CDH).

Extractable Organic Carbon

The extractable organic carbon (EOC) was stable in all of the control soils over the course of the study, ranging from 0.08 to 0.45 mg C per gram dry weight. At the start of the Bloat stage, there was significant increase in EOC in the CDI soils (Figure 18). At the end of Active Decay stage, underneath all of the cadavers except for #50, there was a slight drop in EOC, after which an increase back to the previous concentration was seen shortly afterward. As a whole, EOC was significantly higher in CDI soils compared to control soils until Advanced Decay II stage (Table 3). As with TN, the fate of EOC varied in the Advanced Decay III stage: soils beneath #47 and #50 returned to original levels while the soils beneath #36 and #67 remained high. In all cases the highest EOC values occurred at the same CDH that had the highest TN values.

EOC was significantly correlated to microbial respiration, phosphate, leucine incorporation, ammonia, and total extractable nitrogen, and significantly inversely correlated to microbial growth efficiency (Table 4).

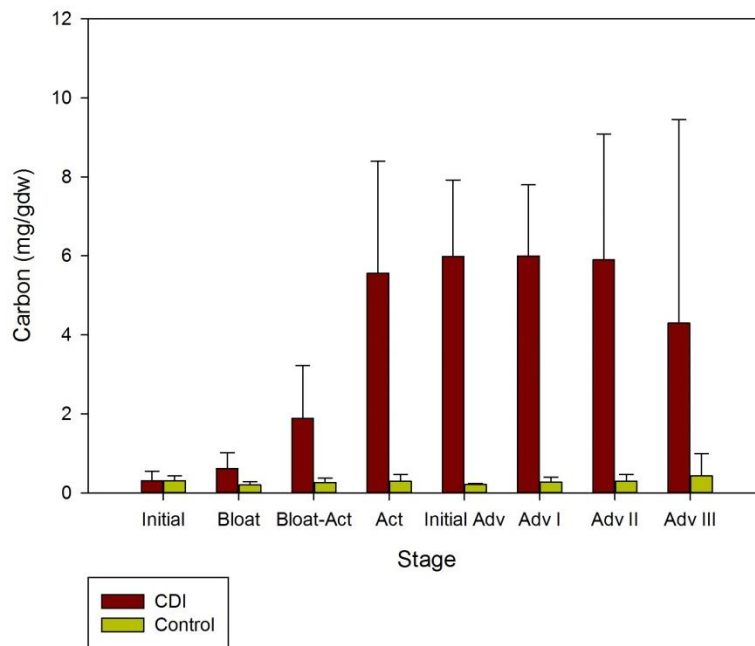


Figure 18. Total extractable organic carbon (EOC) in cadaver decomposition island (CDI) and control soils during decomposition. Abbreviation key as follows: Bloat-Act (Bloat-Active), Act (Active), Initial Adv (Initial Advanced Decay), Adv I (Advanced Decay I), Adv II (Advanced Decay II), Adv III (Advanced Decay III).

Extractable Phosphate

The extractable phosphate concentration in the control soils was negligible, ranging from 0.19 to 0.75 parts per million. Phosphate was not analyzed underneath cadaver #36. Beneath all three cadavers, there was a spike in phosphate concentration as soon as the cadaver was placed, except underneath #50 where the first spike comes later in the Bloat stage (Figure 19). The first peak was followed soon after with a second peak that roughly corresponds to the Active Decay stages of each cadaver. Beneath #50, the phosphate concentration returns to near original levels during the course of this study, while the soil concentrations underneath #47 and #67 remained elevated. Because of the large variability in phosphate concentrations, Advanced Decay II stage was the only stage in which the phosphate concentration was significantly higher than control soils (Table 3). Extractable phosphate was significantly correlated to extractable organic carbon (Table 4).

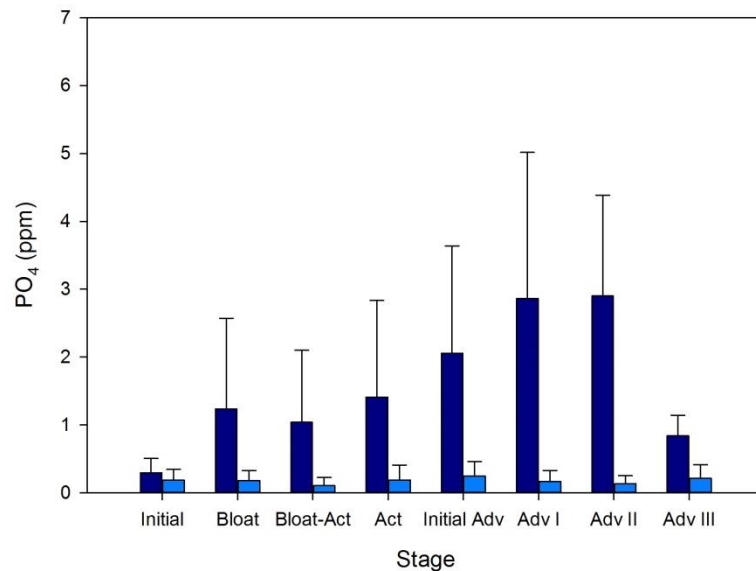


Figure 19. Extractable phosphate concentrations in the cadaver decomposition island (CDI) soils and control soils. Abbreviation key as follows: Bloat-Act (Bloat-Active), Act (Active), Initial Adv (Initial Advanced Decay), Adv I (Advanced Decay I), Adv II (Advanced Decay II), Adv III (Advanced Decay III).

pH

There was no consistent trend in pH for the four replicates (Figure 20). In some cases, CDI soils had elevated pH (#47 and #67), while for the other two cadavers, pH decreased. As a result, there were no significant differences between CDI and control soils for any stage of decomposition (Table 3). Despite the inconsistency between cadavers, pH was significantly correlated to microbial growth efficiency and leucine incorporation (Table 4).

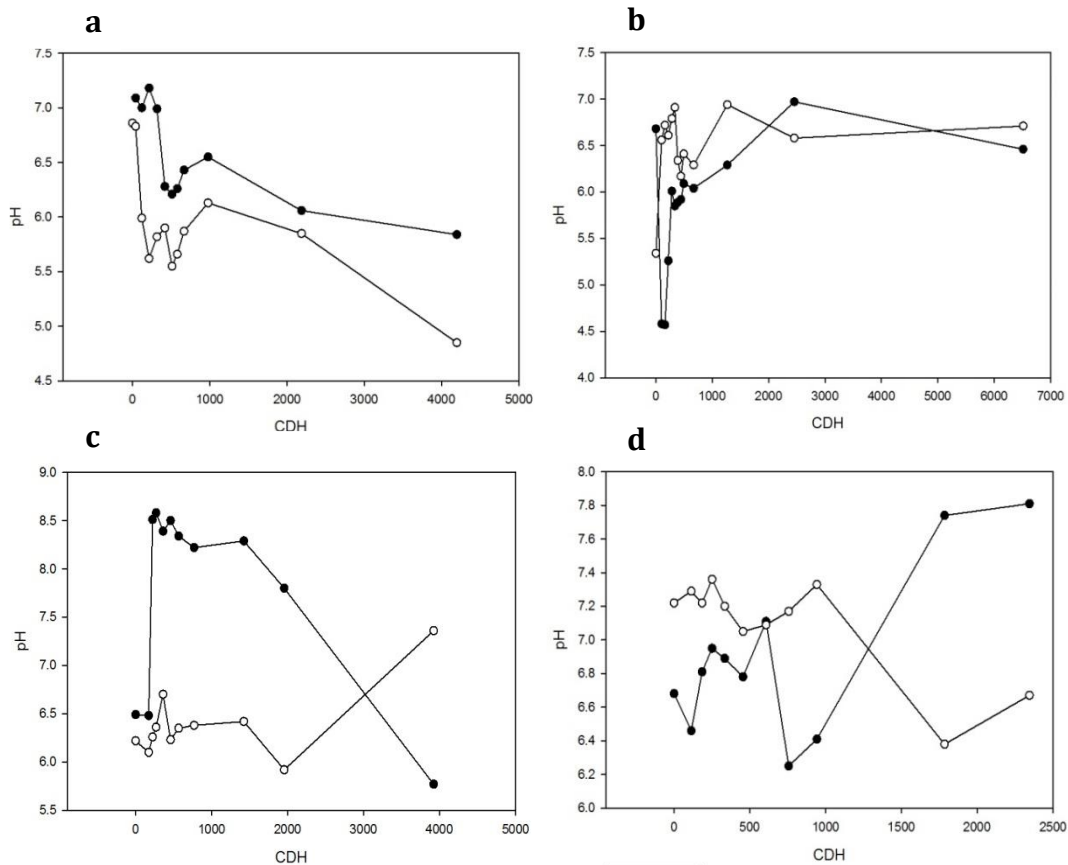


Figure 20. pH in cadaver decomposition island (CDI, filled symbols) and respective control soils (open symbols) for (a) #36, (b) #47, (c) #50, and (d) #67. Data is presented by cumulative degree hours (CDH).

Human-Associated *Bacteroides* 16S rRNA Abundances via qPCR

No human-associated *Bacteroides* (HuBac) 16S rRNA gene copies were detected in the soil samples before placement and during Bloat stage of #47 and #67 (Figure 21b, d). HuBac copies significantly increased at the beginning of Active Decay (Table 4). The site underneath cadaver #50 was discovered to have been previously exposed to HuBac (Figure 21c). Beneath cadaver #36 (Figure 21a), HuBac was detected shortly after placement (but not before), but during the next sampling period, HuBac was not detected. After this initial peak, the trend of the rest of the graph concurred with #47 and #67 graphs. In all CDI soils, copy numbers were significantly elevated starting at the Bloat-Active transition for the duration of the study (Table 3).

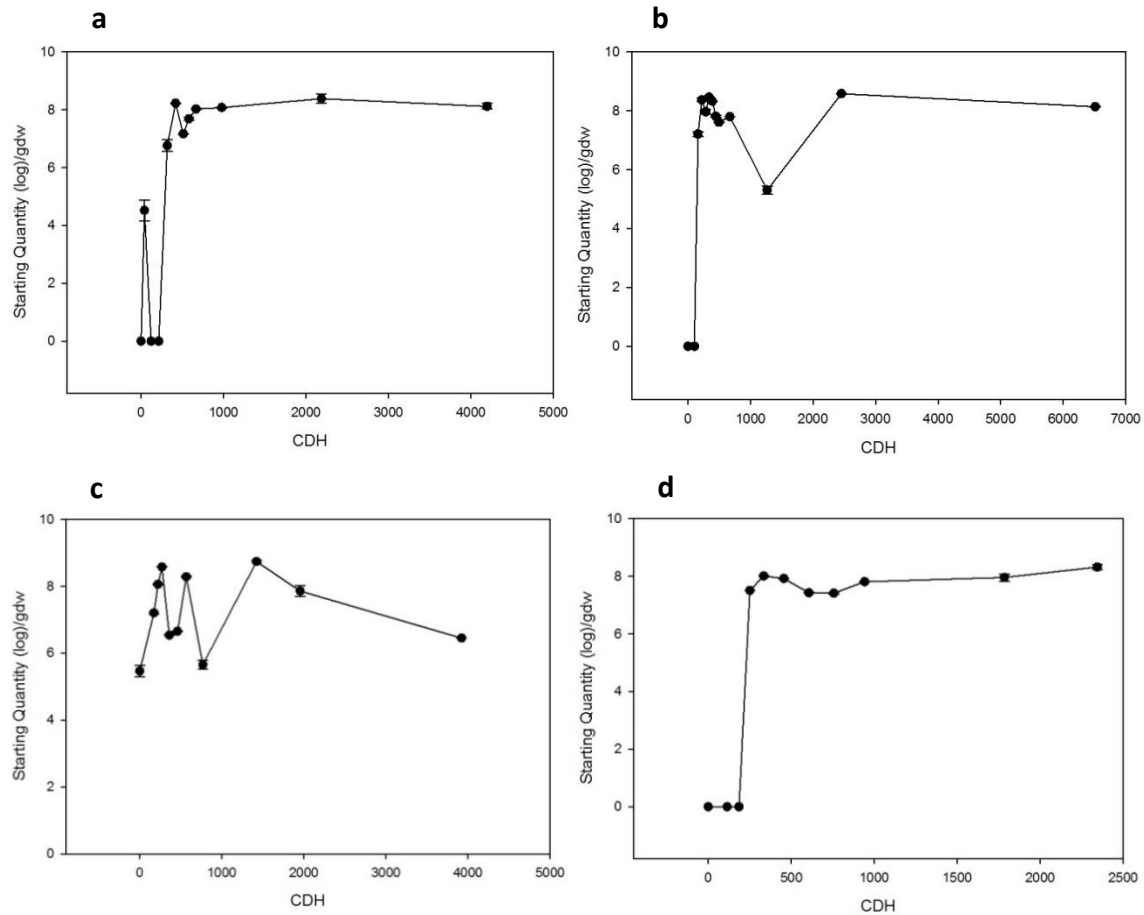


Figure 21. Human-associated *Bacteroides* 16S rRNA gene abundances in soil underneath cadavers (a) #36, (b) #47, (c) #50, and (d) #67. Data is presented by cumulative degree hours (CDH).

Total Bacterial 16S and Fungal ITS region rRNA Abundances via qPCR

Beneath #47 and #50, there was a decline in 16S rRNA copies immediately after the cadaver was placed (data not shown). All of the CDI soils are had a significant increase in 16S rRNA gene copies in Bloat stage and decline in copies in the Active Decay stage (Table 3). Curiously, this decline in copy number in the CDI occurs in Active Decay, when increased respiration was observed. Total 16S rRNA gene copies were positively correlated to leucine incorporation rates (Figure 10).

CHAPTER V

DISCUSSION AND CONCLUSIONS

Microbes play critical roles in a variety of nutrient cycles, such as the carbon and nitrogen cycles. This study focused on the microbial role in organic matter decomposition in a terrestrial ecosystem. This is a key step that links above-ground and below-ground pools of nutrients. Microbial community structure changes following plant litter additions have been extensively investigated, but the decomposition of animal-derived organic matter has often been overlooked. This study examined the microbial community responsible for this process by determining the taxonomic and functional succession in a cadaver decomposition island (CDI). In order to address our objectives, soils from beneath four cadavers at the UT Anthropological Facility were sampled during decomposition. The soil solution was extracted and total nitrogen, ammonia, nitrate, phosphate and organic carbon were measured, as well pH, and soil moisture content. Microbial activity factors, such as biomass production and respiration, were assessed and human-associated *Bacteroides*, total bacterial, and total fungal abundances were measured via qPCR.

During cadaver decay, a few clear patterns emerged. During Bloat-Active Decay stage there was a marked increase in total nitrogen (TN), extractable organic carbon (EOC) and phosphate, corresponding to the influx of decomposition fluids. This increase was observed by other studies as well (Aitkenhead-Peterson et al. 2012; Benninger et al. 2008; Hopkins et al. 2000). All three remained significantly high until Advanced Decay III stage. In comparison to other studies, we observed phosphate concentrations ranging from 0.6-39 $\mu\text{g/gdw}$ and Aitkenhead-Peterson et al. (2012) reported an average of 3.15 $\mu\text{g/gdw}$. For organic carbon, Aitkenhead-Peterson et al. (2012) reported an average of 1.28 mg/gdw, which fell within our range of 0.15-10.1 mg/gdw, but was lower than the average EOC concentration of 3.7 mg/gdw. Discrepancy between the Aitkenhead-Peterson et al. (2012) study and the present study could be due to the differences in the extracting solvent. The previous study used water and we extracted with the salt, potassium chloride. It should be noted that, while the Aitkenhead-Peterson et al. (2012) study also placed human cadavers at the soil surface, Hopkins et al. (2000) buried pig carcasses and Benninger et al. (2008) left pig carcasses to decompose at the soil surface for their studies. We expect little variation in the decomposition process between human cadavers and pig carcasses, only the magnitude of data values should differ (due to mass differences).

Although we cannot compare the scale between this study and that of Benninger et al. (2008), we can still compare trends. They also observed two peaks in phosphate concentrations during the course of their study. Likewise, the current study had a large increase in phosphate, but unlike Benninger et al. (2008) we did not see phosphate concentrations revert to basal levels. One study found elevated phosphorus levels even 39 months later after the decomposition of a mule deer (Parmenter & MacMahon 2009). An anomaly in the phosphate concentration dataset occurred immediately following the placement of the #47 and #67 cadavers: there was a sharp increase in the phosphate concentration in their CDIs during the Fresh stage. Because this occurred before any purge fluids entered the soil, it is believed that a residual cleaning solution on the

cadavers' skin entered the soil solution, but the human skin naturally has phosphorus on it. Normal values range from 450- 980 mg per kg dry defatted weight (Subryan et al. 1975).

One of the clearest observations in this study was the huge increase in total nitrogen (TN) in CDI soils and the largest fraction of TN was ammonia. Very little change in nitrate/nitrite was observed; this suggests that nitrification is not prevalent in the system. Because of similarly high ammonia levels Aitkenhead-Peterson et al. (2012) also hypothesized that nitrification was not occurring in their grave soils. A conceivable hypothesis to explain the lack of nitrate/nitrite is the presence of anaerobic conditions. Clay soils, like those at the ARF, set up a perfect environment for possible anoxic conditions: small pore sizes can slow the draining of water and the exchange of gasses. Under anoxic conditions, decomposition would decrease, volatile fatty acids (VFAs) (via fermentation) and ammonia accumulates, and methane is liberated (Acharya 1935). Vass et al. (1992) reported the presence of VFAs, such as propionic, n-butyric and iso-valeric acids, in the soil solution beneath human cadavers. More evidence for reducing conditions in CDIs was put forth by Hopkins et al. (2000) and Aitkenhead-Peterson et al. (2012): the former observed grey/green tinged soil underneath the carcass (consistent with the reduced forms of iron) and the latter, the lack of or low values of soil sulfate and bicarbonate. Another possibility for the lack of nitrification is the presence of an inhibitor. Various chelating agents, pyridine compounds and even certain amino acids can inhibit ammonia oxidizers (Bedard & Knowles 1989). Another alternative to explain the lack of nitrate/nitrite is denitrification (reduction of nitrate/nitrite to gaseous N_2): denitrification is found to be more active in water-logged anaerobic conditions rather than well-drained soils (Akiyama et al. 2006). Stable isotope probing found that nitrate and succinate were used as an electron acceptor and donor, respectively, for denitrification in rice paddy soils (Saito et al. 2008).

Another observation worth noting is the decline in ammonia (and therefore TN) in Advanced Decay stages II and III in CDI soils under #47 and #50. Vass et al. (1992) saw a similar trend. The reason for this remains unknown, but ammonia volatilization is a possibility. Unfortunately, the evidential support is mixed. The accepted pH cutoff for ammonia volatilization is usually 7.5. The soil beneath #47 ranged from 4.5-7.0 and therefore not conducive to ammonia volatilization. In contrast, the soil under #50 was above 7.5 through much of Advanced Decay stage. Also, there was the slight decrease in TN (largely driven by ammonia) in Initial Advanced Decay; although Benninger et al. (2008) did not assign stages to their data points, this double peak in total nitrogen was also observed in this study. This depression in TN concentration between two peaks coincides with a depression between respiration peaks, further discussed below.

Net nitrogen mineralization is the change in nitrate and ammonia production divided by the change in time, but the nitrate fraction of total N is so minimal that net N mineralization in this case could be thought of as the rate of ammonia production as a byproduct of microbial metabolism. Net N mineralization was not reported in any previous decomposition study. Hopkins et al. (2000) calculated an average net mineralization for the entire study, that ranged from 0.069-1.99 mg/gdw/day for the replicates and it was within the same order of magnitude as the values in this study, which ranged from -0.62-0.87 mg/gdw/day. In natural soils of northern forests, net

nitrogen mineralization ranges from 0.01-250 $\mu\text{g N}$ per gram dry weight of soil per day (Yin et al. 2012; Naples & Fisk 2010; Trap et al. 2009; Boerner et al. 2008; Coates et al. 2008), and our control soils were within this range. The maximum net N mineralization rates observed in the CDI soils was about 400% higher than this 'natural' range. For cadavers #47 and #50, there was considerable variability in rates, possibly due to very warm temperatures during those time periods. Experimental warming experiments showed that increases in temperature significantly increased net N mineralization (Yin et al. 2012; Guntiñas et al. 2012). Dry-wet cycling has also been shown to increase net N mineralization (Q.-H. Chen et al. 2012). The hot temperatures coupled with the intermittent rain during the summer could have mimicked this cycling and caused the fluctuation in mineralization rates. The main trend was an increase in the net N mineralization during the Active Decay stage and subsequent drop in the rate of N mineralization. It should be noted that this observation does not seem to hold in CDI #50 as the increase in net N mineralization begins in the Initial Advanced Decay stage and the scale of mineralization values is one order of magnitude smaller than the rest of the CDIs. The reason for this is unknown.

In this study, we hypothesized that biomass production and respiration would increase rapidly upon introduction of purge fluid and drop once resources deplete. For respiration, this postulate was correct: microbial respiration increased during the onset of decomposition and declined in every CDI except for #36 in the Advanced Decay stages (which could be attributed to a corresponding drop in EOC in CDIs under #47 and #50). In contrast to our hypothesis, microbial biomass production rates initially increased during Bloat-Active stage, but then there was a sharp and significant decrease during Active Decay. Using both biomass production and respiration measurements, we were able to compute microbial growth efficiency (MGE). A sharp drop in MGE immediately occurs after the placement of the cadaver (but before the purge of the bodily fluids) and again in Active Decay stage, despite the fact that studies have found a positive correlation between MGE and phosphorus and dissolved organic carbon in aquatic systems (both of which are high in the CDIs) (Smith & Prairie 2004; Eiler et al. 2003).

One of the most interesting and important trends of the study was the reproducible double peaks in respiration during the Active Decay and Initial Advanced Decay stages, respectively. Since total fungal ITS and bacterial 16S gene copy numbers were not significantly different from the control soils in these stages, it can be inferred that the respiration increases were not caused by an increase in overall microbial population size, but by changes in per cell microbial activity. In combination with the other microbial rates measured, it suggests that the two peaks in respiration correspond to two functionally distinct microbial communities. During the incline and decline of the first peak, there was a similar increase and decrease in biomass production and net N mineralization. Following the first peak in respiration, the reduction in respiration corresponded to the lowest net N mineralization rates. The second peak in respiration, during Advanced Decay, corresponded to no net N mineralization and the MGE was lower than the MGE in during the Active Decay peak. This supports the explanation that two different communities with different N mineralization rates and efficiencies were present. Phylogenetic sequencing is needed to confirm this functional shift.

We can infer that the first increase in respiration is caused by soil copiotrophs utilizing the new labile nutrients in the system. To our knowledge, there are no other studies that have determined respiration as a rate or bacterial biomass production during decomposition. In cumulative measurements, Carter et al. (2008, 2010) reported an increase in cumulative CO₂-C evolution shortly after the placement of skeletal tissue and rat carcasses, respectively, and Carter et al. (2010) noted a decrease in microbial biomass carbon in very wet soils (a matric potential of -0.01 MPa). Due to the narrow C:N of cadaveric material, it might also be beneficial to examine traditional nutrient input studies: high N additions have a negative effect on respiration and bacterial biomass production (E Bååth et al. 1981; Thirukkumaran & Parkinson 2000; F. Demoling et al. 2008; Rousk & Erland Bååth 2007). Demoling et al. (2008) reported decreases up to 44% in bacterial growth rates when ammonium sulfate was added. After the addition of high concentrations of urea or ammonium nitrate, basal respiration decreased (Thirukkumaran & Parkinson 2000). The discrepancy between respiration effects could be attributed to the difference in methods. The microcosms that were set up in our laboratory measured 'potential respiration', as oxygen was artificially introduced before incubation when sieving. Dissimilarly, in the Thirukkumaran et al. (2000) study, for example, they monitored the soil-CO₂ evolution using an infrared gas analyzer in situ. While the MGE in this study range from 0.001-0.9% in the CDI soils, normal soils range from 23% to 63% (Z. M. Lee 2011; Herron et al. 2009; D. S. Schimel 1988). It should be noted that there is no consensus in the discipline on the methods used to determine microbial biomass production (and the conversion factor if applicable) and respiration. Also, the biomass production reported here consists almost entirely of the bacterial fraction. As explained in the methods section, leucine is not incorporated into larger microorganisms like fungi. Most of the values reported in this study are not outside the natural range though: the average bacterial growth efficiency (BGE) in aquatic environments is 15% but some have reported BGEs less than 5% (Eiler et al. 2003; del Giorgio & Cole 1998).

It has been thought that the negative effect of nitrogen on biomass production could be explained by the 'ammonium metabolite repression' phenomenon seen in fungi or an osmotic effect (Thirukkumaran & Parkinson 2000). Ammonia is known to inhibit lignolytic and nitrate-uptake enzyme production in fungi (Arst & Cove 1969); it is possible that this inhibitory effect at very high concentrations also plagues the bacterial community. Growth is also a very sensitive indicator of stress, so there could be a toxic osmotic potential; the detoxification processes could be diverting cellular energy from biomass production. It is also conceivable that the cadaver was emitting an inhibitory compound or an inhibitory metabolic byproduct besides ammonia was building up. Another possibility is that the system reached a physical or nutritional carrying capacity, although the latter appears unlikely given reported high overflow metabolism (high mineralization and respiration rates). The 10¹⁰ 16S rRNA gene copies per gram of soil reported by this study is one to two orders of magnitude higher than the average estimates in forest soils (S. Yarwood et al. 2013; Barta et al. 2010; Kuramae et al. 2012). Unfortunately, to the best of our knowledge, no study has examined the density limits of a terrestrial ecosystem. The decline in MGE at the introduction of purge fluid lends further evidence of soil anoxia, and the absence of the nitrification process. The decrease

in MGE could have been caused by anaerobic conditions in the CDI as the cadaver smothered the soil environment during the first drop and the influx of purge fluid during the second drop. As previously stated, anaerobic respiration and fermentation are not as efficient as aerobic respiration. Further evidence for this theory comes from the fact that MGE increased late in Advanced Decay stage, presumably when most of the purge fluid has leached out of the system and the cadaver mass has decreased.

In our study, we observed no consistency in soil pH during decomposition. There is also no consensus in the literature on pH in grave soils. Some studies have reported an increase (Hopkins et al. 2000; A. S. Wilson et al. 2007; Carter et al. 2010; Rodriguez & Bass 1985; Reed Jr. 1958), decrease (Fiedler et al. 2004), or no significant change (Benninger et al. 2008). The present study results also reflect this variability. Conflicting trends also plagued Aitkenhead-Peterson et al. (2012). One prominent study saw a pH increase during decomposition but then it dropped below basal levels in the long-term (Vass et al. 1992). This trend was consistent with the one in the CDI under #50 (where cadaveric material was found to have been after the study's conclusion) and in a repeat-burial study by Carter et al. (2008).

We hypothesized that the Fungi:Bacteria ratio would increase shortly after the purge fluid entered the soil, then stabilize back to the original ratio upon depletion of nutrients. We reject this hypothesis on the basis that fungal ITS gene copies numbers in the CDI were not significantly higher than the controls. In a similar cadaver study, Parkinson et al. (2009) used the terminal restriction fragment length polymorphism (T-RFLP) method to resolve variations in DNA sequence in the fungal ITS gene to generate a community profile. No clear succession was found over time in the CDI. Although forests are naturally higher in fungal abundances, the control and CDI abundances, which ranged from 8.5-10.7 log/gdw, were at least one order of magnitude higher than previous studies (Kuramae et al. 2012; Jangid et al. 2008). This could be explained by high residual fertility from cadavers placed in the plots before the arrival of GPS-aided mapping of the cadavers at the ARF.

We hypothesized that carcass-associated microbes would enter the soil in the purge fluid and persist in the soil environment until they are outcompeted by the indigenous soil microbes. In this study, we observed the persistence of human-associated *Bacteroides* in high abundance in the CDI soils throughout the entire duration of the experiment. The *Bacteroides* species (of the Bacteroidetes phyla) are anaerobic, non-spore-forming, gram negative rods that enjoy a mutualistic relationship with its host. Together with Firmicutes, Bacteroidetes consist of 95 to 99% of the gut microbiota (Karlsson et al. 2011). No study has examined the survival of the fecal bacterium *Bacteroides* in the soil environment. The literature has predominantly focused on transient pathogenic organisms like *Salmonella* species, *Campylobacter* species and *Escherichia coli* O157. Survival rates varied, as it appeared to depend on (but not limited to) the location of the study (laboratory vs. field), physical properties of the soil (like CEC), bacterial physiology, and soil organic matter (Abu-ashour et al. 1994; Amin et al. 2013). For example, fecal bacteria persist longer in a laboratory microcosm than in situ conditions in general. *Escherichia coli* O157 could survive up to 193 days in the laboratory and up to 99 days under natural conditions (Bolton et al. 1999; Jiang et al. 2002; Gagliardi & Karns 2002). A discrepancy between species seems to exist as well.

Salmonella species and *Campylobacter* species only survived up to 120 and 34 days respectively (Hutchison et al. 2004; Tamasi 1981). Commensals *E.coli* and fecal *Streptococcus* survived up to 160 and 109 days respectively (Ostrolenk, Kramer, & Cleverdon, 1947; Tamasi, 1981). It is important to note that in no previous study did the organism persist in the soil environment; there was always a decline through the course of the investigation. This was attributed in part to predation and competition with the indigenous soil community, for *E.coli* O157 was found to survive much longer in autoclaved, manure amended soils (Jiang et al. 2002).

Due to the absence of comparable studies with *Bacteroides*, we can only speculate on the possible explanation for this persistence. It is likely that a combination of favorable conditions allowed the enteric community to persevere in the soil environment. In general, studies have found that a pH range between five and eight, a soil with high water retention (i.e. clayey soils), and an availability of SOM/ adsorption sites increases survival times of fecal bacteria in soil (Berry & Hagedorn 1991; Abu-ashour et al. 1994). All of these physical conditions are present in the CDIs of this study. Given that *Bacteroides* is obligately anaerobic, another probable CDI trait that favors its survival is anoxic soil conditions. 16S phylogenetic analysis revealed that anoxic rice paddy soil shared species between free-living (like natural soil) and vertebrate gut environments (Ley et al. 2008).

Examination of *Bacteroides*' metabolism in the gut can provide clues whether its nutritional requirements are met in the CDI. A proteomic analysis of the main species *B. fragilis*, revealed a complex system to detect nutrient availability, and a pump system to remove toxic substances (Wexler 2007). Both of these attributes could prove to be beneficial in a soil environment. They also have a multitude of polysaccharide degrading enzymes to digest complex carbohydrates, like starch and cellulose, which human enzymes are unable to break down. Although this study did not specifically measure polysaccharides, it can be assumed from the known biochemistry of the body, these are not in short supply in a CDI. The byproducts of the catabolic breakdown of polysaccharides are VFAs, many of which were found in CDIs as previously mentioned (Vass et al. 1992). The types of VFAs can even give clues as to the species present. For example, the presence of both succinic and iso-butyric acids indicates that *Bacteroides* is there (Baron 1996). Vass et al. (1992) did not detect succinic acid among the water-soluble VFAs found in the soil solution, but iso-butyric acid was present. It is possible that succinate (salt form of succinic acid) is serving as an electron donor in denitrification, or being oxidized in Mn^{4+}/Fe^{3+} sulfate reductions or nitrate respiration (Saito et al. 2008).

With the persistence of a large enteric population, there is cause for concern for public health if leaching into the groundwater occurs. Once in an aquifer, microorganisms have the opportunity to move large distances: fecal coliforms have been reported to move to downstream wells up to 400 feet away depending on the soil type (Gerba 1974). The topography of the ARF might also contribute to bacterial transport: the slope in the facility ranges from 12% to >25% (Damann 2010). Lateral flow between the organic and mineral horizons of the soils, or surface runoff could deposit HuBac into the Tennessee River downslope. Further study needs to be performed to determine the extent (if any) of leaching vertically or laterally in the soil. Also, water-soluble VFAs

created by anaerobic fermentation are mobile and can be harmful through their ability to increase the mobility of heavy metals.

Summary

This study has provided a small glimpse into the decomposition process from the viewpoint of its driving force: the microorganisms. Many questions are left unanswered and many more have been raised by these results. For future work, it will be important to tie the functional processes with phylogenetic identities to further elucidate the shift seen in this study.

LIST OF REFERENCES

- Abu-ashour, J. et al., 1994. Transport of microorganisms through soil. *Water, Air, and Soil Pollution*, 75, pp.141–158.
- Acharya, C.N., 1935. Studies on the anaerobic decomposition of plant materials. III. Comparison of the course of decomposition of rice straw under anaerobic, aerobic and partially aerobic conditions. *Biochemical Journal*, 29(Part 3), pp.1116–1120.
- Aitkenhead-Peterson, J. a et al., 2012. Mapping the lateral extent of human cadaver decomposition with soil chemistry. *Forensic science international*, 216(1-3), pp.127–34. Available at: <http://www.ncbi.nlm.nih.gov/pubmed/21982759> [Accessed January 23, 2013].
- Akiyama, H., Yan, X. & Yagi, K., 2006. Estimations of emission factors for fertilizer-induced direct N₂O emissions from agricultural soils in Japan: Summary of available data. *Soil Science and Plant Nutrition*, 52(6), pp.774–787. Available at: <http://www.tandfonline.com/doi/abs/10.1111/j.1747-0765.2006.00097.x>.
- Allison, S.D. & Martiny, J.B.H., 2008. Resistance, resilience, and redundancy in microbial communities. *Proceedings of the National Academy of Sciences*, 105(Supplement 1), pp.11512–11519. Available at: <http://www.pnas.org/content/105/suppl.1/11512.abstract>.
- Allison, S.D. & Treseder, K.K., 2008. Warming and drying suppress microbial activity and carbon cycling in boreal forest soils. *Global Change Biology*, 14(12), pp.2898–2909.
- Amin, M.G.M. et al., 2013. Persistence and leaching potential of microorganisms and mineral N in animal manure applied to intact soil columns. *Applied and environmental microbiology*, 79(2), pp.535–42. Available at: <http://www.ncbi.nlm.nih.gov/pubmed/23124240> [Accessed March 16, 2013].
- Anon, 2013. Selected weather data. *University of Tennessee Biosystem Engineering and Soil Science*. Available at: <http://bioengr.ag.utk.edu/weather/>.
- Arst, H.N. & Cove, D.J., 1969. Methylammonium Resistance in *Aspergillus nidulans*. *Journal of Bacteriology*, 98 (3), pp.1284–1293. Available at: <http://jb.asm.org/content/98/3/1284.abstract>.
- Avrahami, S., Conrad, R. & Braker, G., 2002. Effect of Soil Ammonium Concentration on N₂O Release and on the Community Structure of Ammonia Oxidizers and Denitrifiers. *Appl. Envir. Microbiol.*, 68(11), pp.5685–5692.
- Bååth, E, Lundgren, B. & Söderström, B., 1981. Effects of nitrogen fertilization on the activity and biomass of fungi and bacteria in a podzolic soil. *Zentralblatt für Bakteriologie Mikrobiologie und Hygiene*, 2(1), pp.90–98. Available at: <http://www.sciencedirect.com/science/article/pii/S072195718180021X>.
- Bååth, E, Pettersson, M. & Soderberg, K.H., 2001. Adaptation of a rapid and economical microcentrifugation method to measure thymidine and leucine incorporation by soil bacteria. *Soil Biology and Biochemistry*, 33(11), pp.1571–1574.

- Baron, S. ed., 1996. *Medical Microbiology* 4th ed., Galveston, TX: University of Texas Medical Branch at Galveston. Available at: <http://www.ncbi.nlm.nih.gov/books/NBK7627/>.
- Barta, J. et al., 2010. Effect of pH and dissolved organic matter on the abundance of nirK and nirS denitrifiers in spruce forest soil. *Biogeochemistry*, 101(1-3), pp.123–132.
- Bedard, C. & Knowles, R., 1989. Physiology, Biochemistry and Specific Inhibitors of CH₄, NH₄ and CO Oxidation by Methanotrophs and Nitrifiers. *Microbiological Reviews*, 53(1), pp.68–84.
- Benninger, L. a, Carter, D.O. & Forbes, Shari L, 2008. The biochemical alteration of soil beneath a decomposing carcass. *Forensic science international*, 180(2-3), pp.70–5. Available at: <http://www.ncbi.nlm.nih.gov/pubmed/18752909> [Accessed July 24, 2011].
- Berg, B. & McLaugherty, C., 2008. Litter Decomposition – a Set of Different Processes. In *Plant Litter*. Springer-Verlag Berlin Heidelberg, pp. 11–33.
- Berry, D.F. & Hagedorn, C., 1991. Soil and Groundwater Transport of Microorganisms. In L. R. Ginzburg, ed. *Assessing ecological risks of biotechnology*. Reading, Mass.: Butterworth-Heinemann, pp. 57–73.
- Bitton, G., Lahav, N. & Henis, Y., 1974. Movement and retention of Klebsiella aerogenes in soil columns. *Plant and Soil*, 40(2), pp.373–380. Available at: <http://dx.doi.org/10.1007/BF00011519>.
- Van Bodegom, P., 2007. Microbial maintenance: a critical review on its quantification. *Microbial ecology*, 53(4), pp.513–23. Available at: <http://www.pubmedcentral.nih.gov/articlerender.fcgi?artid=1915598&tool=pmcentrez&rendertype=abstract> [Accessed February 9, 2013].
- Boerner, R.E.J. et al., 2008. Initial effects of fire and mechanical thinning on soil enzyme activity and nitrogen transformations in eight North American forest ecosystems. *Soil Biology and Biochemistry*, 40(12), pp.3076–3085. Available at: <http://www.sciencedirect.com/science/article/pii/S0038071708003167>.
- Bolton, D.J. et al., 1999. The survival characteristics of a non-toxicogenic strain of Escherichia coli O157 : H7. *Journal of Applied Microbiology*, 86(3), pp.407–411.
- Brady, N.C. & Weil, R.R., 2008. *The Nature and Properties of Soils* 14th ed., Upper Saddle River, NJ: Pearson-Prentice Hall.
- Carter, D.O. & Tibbett, M., 2008. Does repeated burial of skeletal muscle tissue (Ovis aries) in soil affect subsequent decomposition? *Applied Soil Ecology*, 40(3), pp.529–535. Available at: <http://linkinghub.elsevier.com/retrieve/pii/S0929139308001315> [Accessed September 17, 2011].

- Carter, D.O., Yellowlees, D. & Tibbett, M., 2007. Cadaver decomposition in terrestrial ecosystems. *Die Naturwissenschaften*, 94(1), pp.12–24. Available at: <http://www.ncbi.nlm.nih.gov/pubmed/17091303> [Accessed August 9, 2011].
- Carter, D.O., Yellowlees, D. & Tibbett, M., 2010. Moisture can be the dominant environmental parameter governing cadaver decomposition in soil. *Forensic Science International*, 200(1-3), pp.60–66.
- Chapin, F.S. et al., 2000. Consequences of changing biodiversity. *Nature*, 405(6783), pp.234–242. Available at: <http://www.ncbi.nlm.nih.gov/pubmed/10821284>.
- Chen, Q.-H. et al., 2012. Short-Term Responses of Nitrogen Mineralization and Microbial Community to Moisture Regimes in Greenhouse Vegetable Soils. *Pedosphere*, 22(2), pp.263–272. Available at: <http://www.sciencedirect.com/science/article/pii/S1002016012600137>.
- Child, A.M., 1995. Towards an Understanding of the Microbial Decomposition of Archaeological Bone in the Burial Environment. *Journal of Archaeological Science*, pp.165–174.
- Cleveland, C. & Liptzin, D., 2007. C:N:P stoichiometry in soil: is there a “Redfield ratio” for the microbial biomass? *Biogeochemistry*, 85(3), pp.235–252. Available at: <http://dx.doi.org/10.1007/s10533-007-9132-0>.
- Coates, T.A. et al., 2008. Soil Nitrogen Transformations Under Alternative Management Strategies in Appalachian Forests All rights reserved. No part of this periodical may be reproduced or transmitted in any form or by any means, electronic or mechanical, including photocopying, re. , 72(2), pp.558–565. Available at: <https://www.soils.org/publications/sssaj/abstracts/72/2/558>.
- Costello, E.K. et al., 2009. Bacterial community variation in human body habitats across space and time. *Science*, 326(5960), pp.1694–7. Available at: <http://www.ncbi.nlm.nih.gov/pubmed/19892944> [Accessed July 6, 2011].
- Damann, F.E., 2010. *Human Decomposition Ecology at the University of Tennessee Anthropology Research Facility*. University of Tennessee.
- Demoling, F., Nilsson, L.O. & Bååth, Erland, 2008. Bacterial and fungal response to nitrogen fertilization in three coniferous forest soils. *Soil Biology and Biochemistry*, 40(2), pp.370–379. Available at: <http://www.sciencedirect.com/science/article/pii/S0038071707003549>.
- Dent, Forbes, S. L. & Stuart, B.H., 2004. Review of human decomposition processes in soil. *Environmental Geology*, 45(4), pp.576–585. Available at: <http://www.springerlink.com/openurl.asp?genre=article&id=doi:10.1007/s00254-003-0913-z> [Accessed June 17, 2011].
- Desprez-Loustau, M.-L. et al., 2007. The fungal dimension of biological invasions. *Trends in ecology & evolution*, 22(9), pp.472–80. Available at: <http://www.ncbi.nlm.nih.gov/pubmed/17509727> [Accessed November 9, 2012].

- Eiler, A. et al., 2003. Heterotrophic Bacterial Growth Efficiency and Community Structure at Different Natural Organic Carbon Concentrations. *Applied and Environmental Microbiology*, 69 (7), pp.3701–3709. Available at: <http://aem.asm.org/content/69/7/3701.abstract>.
- Van Elsas, J.D. et al., 2011. Survival of *Escherichia coli* in the environment: fundamental and public health aspects. *The ISME journal*, 5(2), pp.173–83. Available at: <http://www.ncbi.nlm.nih.gov/pubmed/20574458> [Accessed July 26, 2011].
- Essington, M.E., 2004. *Soil and Water Chemistry: An Integrative Approach*, Boca Raton, FL.: CRC Press.
- Fiedler, S., Schneckengerber, K. & Graw, M., 2004. Characterization of Soils Containing Adipocere. *Archives of Environmental Contamination and Toxicology*, 47(4), pp.561–568. Available at: <http://dx.doi.org/10.1007/s00244-004-3237-4>.
- Fierer, N. et al., 2005. Assessment of Soil Microbial Community Structure by Use of Taxon-Specific Quantitative PCR Assays. *Applied and environmental microbiology*, 71(7), pp.4117–4120.
- Fierer, N., Bradford, M. a & Jackson, R.B., 2007. Toward an ecological classification of soil bacteria. *Ecology*, 88(6), pp.1354–64. Available at: <http://www.ncbi.nlm.nih.gov/pubmed/17601128>.
- Fontaine, S. et al., 2004. Carbon input to soil may decrease soil carbon content. *Ecology Letters*, 7(4), pp.314–320. Available at: <http://doi.wiley.com/10.1111/j.1461-0248.2004.00579.x> [Accessed February 4, 2013].
- Fontaine, S., Mariotti, A. & Abbadie, L., 2003. The priming effect of organic matter: a question of microbial competition? *Soil Biology and Biochemistry*, 35(6), pp.837–843. Available at: <http://linkinghub.elsevier.com/retrieve/pii/S0038071703001238> [Accessed January 31, 2013].
- G J Olsen, et al., 2003. Microbial Ecology and Evolution: A Ribosomal RNA Approach. Available at: <http://www.annualreviews.org/doi/abs/10.1146/annurev.mi.40.100186.002005> [Accessed January 24, 2013].
- Gagliardi, J. V & Karns, J.S., 2002. Persistence of *Escherichia coli* O157:H7 in soil and on plant roots. *Environmental microbiology*, 4(2), pp.89–96. Available at: <http://www.ncbi.nlm.nih.gov/pubmed/11972618>.
- Gardes, M. & Bruns, T., 1993. ITS primers with enhanced specificity for basidiomycetes-- application to the identification of mycorrhizae and rusts. *Molecular Ecology*, 2(2), pp.113–118.
- Gerba, C.P., 1974. *The Fate of Wastewater Bacteria and Viruses in the Soil*, Baylor College of Medicine. Available at: <http://books.google.com/books?id=POleYgEACAAJ>.

- Gill, S.R. et al., 2006. Metagenomic analysis of the human distal gut microbiome. *Science (New York, N.Y.)*, 312(5778), pp.1355–9. Available at: <http://www.pubmedcentral.nih.gov/articlerender.fcgi?artid=3027896&tool=pmcentrez&rendertype=abstract> [Accessed March 4, 2013].
- Del Giorgio, P.A. & Cole, J.J., 1998. Bacterial growth efficiency in natural aquatic systems. *Annual Review of Ecology and Systematics*, 29(1), pp.503–541. Available at: <http://www.annualreviews.org/doi/abs/10.1146/annurev.ecolsys.29.1.503>.
- Griffiths, B.S. et al., 1998. Ryegrass rhizosphere microbial community structure under elevated carbon dioxide concentrations, with observations on wheat rhizosphere. *Soil Biology and Biochemistry*, 30(3), pp.315–321. Available at: <http://www.sciencedirect.com/science/article/pii/S0038071797001338>.
- Griffiths, B.S. et al., 1999. Soil microbial community structure: Effects of substrate loading rates. *Soil Biology and Biochemistry*, 31(1), pp.145–153.
- Gutiñas, M.E. et al., 2012. Effects of moisture and temperature on net soil nitrogen mineralization: A laboratory study. *European Journal of Soil Biology*, 48(0), pp.73–80. Available at: <http://www.sciencedirect.com/science/article/pii/S1164556311000732>.
- Herron, P.M. et al., 2009. Microbial growth efficiencies across a soil moisture gradient assessed using ¹³C-acetic acid vapor and ¹⁵N-ammonia gas. *Soil Biology and Biochemistry*, 41(6), pp.1262–1269. Available at: <http://linkinghub.elsevier.com/retrieve/pii/S0038071709001187> [Accessed March 17, 2013].
- Hicks, R.E., Amann, R.I. & Stahl, D.A., 1992. Dual staining of natural bacterioplankton with 4',6-diamidino-2-phenylindole and fluorescent oligonucleotide probes targeting kingdom-level 16S rRNA sequences. *Appl. Envir. Microbiol.*, 58(7), pp.2158–2163. Available at: <http://aem.asm.org/content/58/7/2158> [Accessed January 24, 2013].
- Hill, M.J., 1997. Intestinal flora and endogenous vitamin synthesis. *European Journal of Cancer Prevention*, 6, pp.S43–5.
- Hopkins, D.W., Wiltshire, P.E.J. & Turner, B.D., 2000. Microbial characteristics of soils from graves : an investigation at the interface of soil microbiology and forensic science. *Applied Soil Ecology*, 14, pp.283–288.
- Horwath, W., 2007. Carbon Cycling and Formation of Soil Organic Matter. In P. Eldor, ed. *Soil microbiology, ecology, and biochemistry*. Elsevier, pp. 303–337.
- Howard, G.T., Duos, B. & Watson-Horzelski, E.J., 2010. Characterization of the soil microbial community associated with the decomposition of a swine carcass. *International Biodeterioration & Biodegradation*, 64(4), pp.300–304. Available at: <http://linkinghub.elsevier.com/retrieve/pii/S0964830510000363> [Accessed September 18, 2011].

- Hutchison, M.L. et al., 2004. Effect of Length of Time before Incorporation on Survival of Pathogenic Bacteria Present in Livestock Wastes Applied to Agricultural Soil. *Applied and environmental microbiology*, 70(9).
- Jangid, K. et al., 2008. Relative impacts of land-use, management intensity and fertilization upon soil microbial community structure in agricultural systems. *Soil Biology and Biochemistry*, 40(11), pp.2843–2853. Available at: <http://www.sciencedirect.com/science/article/pii/S0038071708002745>.
- Jans-Hammermeister, D.C., McGill, W.B. & Izaurralde, R.C., 1997. Management of Soil C by Manipulation of Microbial Metabolism: Daily vs. Pulse C Additions. In R. Lal et al., eds. *Soil Processes and the Carbon Cycle*. Boca Raton, FL.: CRC Press, pp. 321–334.
- Janssen, P.H., 2006. Identifying the Dominant Soil Bacterial Taxa in Libraries of 16S rRNA and 16S rRNA Genes. *Applied and Environmental Microbiology*, 72(3), pp.1719–1728. Available at: <http://aem.asm.org/content/72/3/1719.short>.
- Jenkinson, D.S., 1977. STUDIES ON DECOMPOSITION OF PLANT MATERIAL IN SOIL 4. EFFECT OF RATE OF ADDITION. *The Journal of Soil Science*, 28(3), pp.417–423.
- Jiang, X., Morgan, J. & Doyle, M.P., 2002. Fate of Escherichia coli O157 : H7 in Manure-Amended Soil. *Appl. Envir. Microbiol.*, 68(5), pp.2605–2609.
- Johnson, D., 1992. Effects of forest management on soil carbon storage. *Water, Air, and Soil Pollution*, 64(1-2), pp.83–120. Available at: <http://dx.doi.org/10.1007/BF00477097>.
- Karlovsky, P. ed., 2008. *Secondary Metabolites in Soil Ecology*, Springer.
- Karlsson, F.H. et al., 2011. A closer look at bacteroides: phylogenetic relationship and genomic implications of a life in the human gut. *Microbial ecology*, 61(3), pp.473–85. Available at: <http://www.ncbi.nlm.nih.gov/pubmed/21222211> [Accessed March 16, 2013].
- Kemmitt, S.J. et al., 2008. Mineralization of native soil organic matter is not regulated by the size, activity or composition of the soil microbial biomass—a new perspective. *Soil Biology and Biochemistry*, 40(1), pp.61–73. Available at: <http://www.sciencedirect.com/science/article/pii/S0038071707002891>.
- Killham, K. & Prosser, J.I., 2007. The Prokaryotes. In P. Eldor, ed. *Soil microbiology, ecology, and biochemistry*. Elsevier, pp. 119–143.
- Kirchman, D., 2001. 12 Measuring Bacterial Biomass Production and Growth Rates from Leucine Incorporation in Natural Aquatic Environments.
- Klappenbach, J.A., Dunbar, J.M. & Schmidt, T.M., 2000. RRNA operon copy number reflects ecological strategies of bacteria. *Applied and Environmental Microbiology*, 66(4), pp.1328–1333.

- Kuramae, E.E. et al., 2012. Soil characteristics more strongly influence soil bacterial communities than land-use type. *FEMS Microbiology Ecology*, 79(1), pp.12–24. Available at: <http://dx.doi.org/10.1111/j.1574-6941.2011.01192.x>.
- Layton, A. et al., 2006. Development of Bacteroides 16S rRNA gene TaqMan-based real-time PCR assays for estimation of total, human, and bovine fecal pollution in water. *Applied and environmental microbiology*, 72(6), pp.4214–4224.
- Van der Lee, G. et al., 1999. Anoxic microsites in Douglas fir litter. *Soil Biology and Biochemistry*, 31, pp.1295–1301.
- Lee Wise, D., 2000. *Bioremediation of Contaminated Soils*, CRC Press.
- Lee, Z.M., 2011. *Bacterial growth efficiency: assessment in terrestrial ecosystems*. Michigan State University.
- Ley, R.E. et al., 2008. Worlds within worlds: evolution of the vertebrate gut microbiota. *Nature reviews. Microbiology*, 6(10), pp.776–88. Available at: <http://www.pubmedcentral.nih.gov/articlerender.fcgi?artid=2664199&tool=pmcentrez&rendertype=abstract>.
- Likens, G.E., Driscoll, C.T. & Buso, D.C., 2013. Long-Term Effects of Acid Rain : Response and Recovery of a Forest Ecosystem. , 272(5259), pp.244–246.
- Lipson, D.A., Wilson, R.F. & Oechel, W.C., 2005. Effects of elevated atmospheric CO₂ on soil microbial biomass, activity, and diversity in a chaparral ecosystem. *Applied and environmental microbiology*, 71(12), pp.8573–8580.
- MacArthur, R.H. & Wilson, E.O., 1967. *The Theory of Island Biogeography*, New Jersey: Princeton University Press.
- Mann, R.W., Bass, W.M. & Meadows, L., 1990. Time since death and decomposition of the human body: variables and observations in case and experimental field studies. *Journal of forensic sciences*, 35(1), pp.103–11. Available at: <http://www.ncbi.nlm.nih.gov/pubmed/2313251>.
- Marshall, K.C., 1971. Mechanism of initial events in sorption of marine bacteria to surfaces. *Journal of General Microbiology*, 68.
- Martin-Laurent, F. et al., 2001. DNA extraction from soils: Old bias for new microbial diversity analysis methods. *Applied and Environmental Microbiology*, 67(5), pp.2354–2359.
- McClain, M.E. et al., 2003. Biogeochemical Hot Spots and Hot Moments at the Interface of Terrestrial and Aquatic Ecosystems. *Ecosystems*, 6(4), pp.301–312. Available at: <http://link.springer.com/10.1007/s10021-003-0161-9> [Accessed January 31, 2013].
- Michel, P.H. & Bloem, J., 1993. Conversion factors for estimation of cell production rates of soil bacteria from [3H]thymidine and [3H]leucine incorporation. *Soil Biology and Biochemistry*,

25(7), pp.943–950. Available at:
<http://www.sciencedirect.com/science/article/pii/S003807179390097U>.

Morris, S.J. & Blackwood, C.B., 2007. The Ecology of Soil Organisms. In P. Eldor, ed. *Soil microbiology, ecology, and biochemistry*. Elsevier, pp. 195–226.

Müller, T. & Höper, H., 2004. Soil organic matter turnover as a function of the soil clay content: consequences for model applications. *Soil Biology and Biochemistry*, 36(6), pp.877–888. Available at: <http://linkinghub.elsevier.com/retrieve/pii/S0038071704000471> [Accessed January 20, 2013].

Naeem, S. & Li, S., 1997. Biodiversity enhances ecosystem reliability. *Nature*, 390(6659), pp.507–509. Available at: <http://dx.doi.org/10.1038/37348>.

Naples, B. & Fisk, M., 2010. Belowground insights into nutrient limitation in northern hardwood forests. *Biogeochemistry*, 97(2-3), pp.109–121. Available at: <http://dx.doi.org/10.1007/s10533-009-9354-4>.

NCSS, 2004. *Soil Survey of Knox County, Tennessee*,

Niklaus, P.A. et al., 2003. Six years of in situ CO₂ enrichment evoke changes in soil structure and soil biota of nutrient-poor grassland. *Global Change Biology*, 9(4), pp.585–600.

Ostrolenk, M., Kramer, N. & Cleverdon, R.C., 1947. Comparative Studies of Enterococci and Escherichia coli as Indices of Pollution. *Journal of bacteriology*, 53(2), pp.197–203. Available at: <http://www.pubmedcentral.nih.gov/articlerender.fcgi?artid=518293&tool=pmcentrez&rendertype=abstract>.

Padmanabhan, P. et al., 2003. Respiration of ¹³C-Labeled Substrates Added to Soil in the Field and Subsequent 16S rRNA Gene Analysis of ¹³C-Labeled Soil DNA. *Applied and Environmental Microbiology*, 69(3), pp.1614–1622. Available at: <http://aem.asm.org/content/69/3/1614.abstract>.

Parkin, T.B., 1987. Soil microsites as a source of denitrification variability. *Soil Science Society of America Journal*, 51(5), pp.1194 –1199.

Parmenter, R. & MacMahon, J., 2009. Carrion decomposition and nutrient cycling in a semiarid shrub – steppe ecosystem. *Ecological Monographs*, 79(4), pp.637–661.

Paul, E.A., Collins, H.P. & Leavitt, S.W., 2001. Dynamics of resistant soil carbon of Midwestern agricultural soils measured by naturally occurring ¹⁴C abundance. *Geoderma*, 104(3–4), pp.239–256. Available at: <http://www.sciencedirect.com/science/article/pii/S0016706101000830>.

Payne, J.A., 1965. A Summer Carrion Study of the Baby Pig Sus Scrofa Linnaeus. *Ecological Society of America*, 46(5), pp.592–602.

- Perroni-Ventura, Y., Montana, C. & Garcia-Oliva, F., 2010. Carbon-nitrogen interactions in fertility island soil from a tropical semi-arid ecosystem. *Functional Ecology*, 24(1), pp.233–242. Available at: <http://doi.wiley.com/10.1111/j.1365-2435.2009.01610.x> [Accessed January 25, 2013].
- Poindexter, J.S., 1981. Oligotrophy: Fast and famine existence. *Advances in Microbial Ecology*, 1(5), pp.63–90.
- Pollan, M., 2006. Gathering: The Fungi. In *The Omnivore's Dilemma*. New York, New York: Penguin Group (USA) Inc., p. 376.
- Van der Putten, W.H., Klironomos, J.N. & Wardle, D. a, 2007. Microbial ecology of biological invasions. *The ISME journal*, 1(1), pp.28–37. Available at: <http://www.ncbi.nlm.nih.gov/pubmed/18043611> [Accessed November 2, 2012].
- R Core Team, 2012. *R: A Language and Environment for Statistical Computing*, Vienna, Austria. Available at: <http://www.r-project.org/>.
- Rahe, T.M., 1978. Transport of antibiotic-resistant escherichia-coli through western oregon hillslope soils under conditions of saturated flow. *Journal of environmental quality*, 7(4), pp.487–494.
- Raich, J.W. & Schlesinger, W.H., 1992. The global carbon-dioxide flux in soil respiration and its relationship to vegetation and climate. *Tellus Series B-chemical And Physical Meteorology*, 44(2), pp.81–99.
- Rail, C.D., 2000. *Groundwater Contamination: Contamination, sources & hydrology*, CRC Press.
- Reed Jr., H.B., 1958. A Study of Dog Carcass Communities in Tennessee, with Special Reference to the Insects. *American Midland Naturalist*, 59(1), pp.213–245. Available at: <http://www.jstor.org/stable/2422385>.
- Reed, H.E. & Martiny, J.B.H., 2007. Testing the functional significance of microbial composition in natural communities. *FEMS microbiology ecology*, 62(2), pp.161–70. Available at: <http://www.ncbi.nlm.nih.gov/pubmed/17937673> [Accessed February 2, 2013].
- Reid, A., 2011. *Incorporating microbial processes into climate models*, Available at: http://academy.asm.org/images/stories/documents/Incorporating_Microbial_Processes_Into_Climate_Models.pdf.
- Ridolfi, L., Laio, F. & Odorico, P.D., 2008. Fertility Island Formation and Evolution in Dryland Ecosystems. *Ecology and Society*, 13(1).
- Robertson, G. & Groffman, P., 2007. Nitrogen Transformations. In P. Eldor, ed. *Soil microbiology, ecology, and biochemistry*. Elsevier, pp. 341–362.

- Rodriguez, W.C. & Bass, W.M., 1985. Decomposition of buried bodies and methods that may aid in their location. *Journal of forensic sciences*, 30(3), pp.836–52. Available at: <http://www.ncbi.nlm.nih.gov/pubmed/4031811>.
- Rousk, J. et al., 2008. Examining the fungal and bacterial niche overlap using selective inhibitors in soil. *FEMS microbiology ecology*, 63(3), pp.350–8. Available at: <http://www.ncbi.nlm.nih.gov/pubmed/18205814> [Accessed February 4, 2013].
- Rousk, J. & Bååth, Erland, 2007. Fungal and bacterial growth in soil with plant materials of different C/N ratios. *FEMS microbiology ecology*, 62(3), pp.258–67. Available at: <http://www.ncbi.nlm.nih.gov/pubmed/17991019> [Accessed February 4, 2013].
- Saito, T. et al., 2008. Identification of Novel *Betaproteobacteria* in a Succinate-Assimilating Population in Denitrifying Rice Paddy Soil by Using Stable Isotope Probing. *Microbes and Environments*, 23(3), pp.192–200.
- Schimel, D.S., 1988. Calculation of Microbial Growth Efficiency from ¹⁵N Immobilization. *Biogeochemistry*, 6(3), pp.239–243. Available at: <http://www.jstor.org/stable/1468515>.
- Schimel, J. P., Balsler, T.C., & Matthew, W., 2007. Microbial Stress-Response Physiology and Its Implications for Ecosystems. *Ecological Society of America*, 88(6), pp.1386–1394.
- Schimel, J. & Weintraub, M., 2003. The implications of exoenzyme activity on microbial carbon and nitrogen limitation in soil: a theoretical model. *Soil Biology and Biochemistry*, 35(4), pp.549–563. Available at: <http://linkinghub.elsevier.com/retrieve/pii/S0038071703000154> [Accessed November 10, 2012].
- Schimel, Joshua P & Chapin F. Stuart, I.I.I., 1996. Tundra Plant Uptake of Amino Acid and NH₄ + Nitrogen in Situ: Plants Complete Well for Amino Acid N. *Ecology*, 77(7), pp.2142–2147. Available at: <http://www.jstor.org/stable/2265708>.
- Scott, N.A., 1996. Soil textural control on decomposition and soil organic matter dynamics. *Soil Science Society of America Journal*, 60(4), pp.1102–1109.
- Smith, E.M. & Prairie, Y.T., 2004. Bacterial metabolism and growth efficiency in lakes: The importance of phosphorus availability. *Limnology and Oceanography*, 49(1), pp.137–147.
- Sonnemann, I. & Wolters, V., 2005. The microfood web of grassland soils responds to a moderate increase in atmospheric CO₂. *Global Change Biology*, 11(7), pp.1148–1155.
- Stevenson, F., 1994. *Humus Chemistry – Genesis, Composition Reactions*, New York: Wiley.
- Strickland, M.S., Osburn, E., et al., 2009. Litter quality is in the eye of the beholder: initial decomposition rates as a function of inoculum characteristics. *Functional Ecology*, 23(3), pp.627–636. Available at: <http://doi.wiley.com/10.1111/j.1365-2435.2008.01515.x> [Accessed January 29, 2013].

- Strickland, M.S., Lauber, C., et al., 2009. Testing the functional significance of microbial community composition. *Ecology*, 90(2), pp.441–51. Available at: <http://www.ncbi.nlm.nih.gov/pubmed/19323228>.
- Subryan, V.L. et al., 1975. A micromethod for the quantitative analysis of calcium, magnesium, and phosphorus in human skin. *The Journal of laboratory and clinical medicine*, 86(6), pp.1056–1060. Available at: <http://europepmc.org/abstract/MED/1194753>.
- Tamasi, G., 1981. Factors Influencing the Survival of Pathogenic Bacteria in Soils. *Acta veterinaria*, 29(2), pp.119–126.
- Tate, R.L., 1979. Microbial activity in organic soils as affected by soil depth and crop. *Applied and environmental microbiology*, 37(6), pp.1085–90. Available at: <http://www.pubmedcentral.nih.gov/articlerender.fcgi?artid=243358&tool=pmcentrez&rendertype=abstract>.
- Thirukkumaran, C.M. & Parkinson, D., 2000. Microbial respiration, biomass, metabolic quotient and litter decomposition in a lodgepole pine forest floor amended with nitrogen and phosphorous fertilizers. *Soil Biology and Biochemistry*, 32(1), pp.59–66. Available at: <http://www.sciencedirect.com/science/article/pii/S0038071799001297>.
- Torsvik, V. et al., 1998. Novel techniques for analysing microbial diversity in natural and perturbed environments. *Journal Of Biotechnology*, 64(1), pp.53–62.
- Towne, E., 2000. Prairie vegetation and soil nutrient responses to ungulate carcasses. *Oecologia*, 122(2), pp.232–239.
- Trap, J. et al., 2009. Changes in soil N mineralization and nitrification pathways along a mixed forest chronosequence. *Forest Ecology and Management*, 258(7), pp.1284–1292. Available at: <http://www.sciencedirect.com/science/article/pii/S0378112709004265>.
- Vass, A.A. et al., 2002. Decomposition chemistry of human remains: a new methodology for determining the postmortem interval. *Journal of forensic sciences*, 47(3), pp.542–53. Available at: <http://www.ncbi.nlm.nih.gov/pubmed/12051334>.
- Vass, A.A. et al., 1992. Time since death determinations of human cadavers using soil solution. *Journal of forensic sciences*, 37(5), pp.1236–53. Available at: <http://www.ncbi.nlm.nih.gov/pubmed/1402750>.
- Vilgalys, R & Hester, M., 1990. Rapid genetic identification and mapping of enzymatically amplified ribosomal DNA from several cryptococcus species. *Journal Of Bacteriology*, 172(8), pp.4238–4246.
- Walker, F. et al., 2012. Leachate Analysis from an Organic Burial Pit Containing Euthanized Large Animals. In *ASA, CSA, and SSSA International Annual Meetings, Cincinnati, OH*.
- Weber, C.A., 1907. Aufbau and vegetatioin der moore norddeutschlands. *Beiblatt zu den Botanischen*, 90, pp.19–34.

- Wexler, H.M., 2007. Bacteroides: the good, the bad, and the nitty-gritty. *Clinical microbiology reviews*, 20(4), pp.593–621. Available at: <http://www.pubmedcentral.nih.gov/articlerender.fcgi?artid=2176045&tool=pmcentrez&rendertype=abstract> [Accessed February 27, 2013].
- Wheeler, K.A., Hurdman, B.F. & Pitt, J.I., 1991. Influence of pH on the growth of some toxigenic species of aspergillus, penicillium and fusarium. *International Journal Of Food Microbiology*, 12(2-3), pp.141–150.
- Wickham, H., 2009. *ggplot2: elegant graphics for data analysis*, Springer New York. Available at: <http://had.co.nz/ggplot2/book>.
- Wilson, A.S. et al., 2007. Modelling the buried human body environment in upland climes using three contrasting field sites. *Forensic science international*, 169(1), pp.6–18. Available at: <http://www.ncbi.nlm.nih.gov/pubmed/16973322> [Accessed August 1, 2011].
- Winogradsky, S., 1924. Sur la microflora autochthone de la terrearable. *Hebd Acad Sci*, 178, pp.1236–1239.
- Yarwood, S. et al., 2013. Soil Microbe Active Community Composition and Capability of Responding to Litter Addition after 12 Years of No Inputs. *Applied and Environmental Microbiology*, 79 (4), pp.1385–1392. Available at: <http://aem.asm.org/content/79/4/1385.abstract>.
- Yin, H., Chen, Z. & Liu, Q., 2012. Effects of experimental warming on soil N transformations of two coniferous species, Eastern Tibetan Plateau, China. *Soil Biology and Biochemistry*, 50(0), pp.77–84. Available at: <http://www.sciencedirect.com/science/article/pii/S0038071712001058>.
- Zogg, G.P. et al., 1997. Compositional and functional shifts in microbial communities due to soil warming. *Soil Science Society of America Journal*, 61(2), pp.475–481.

APPENDIX

Table A1. Decomposition stage at each sampling day. The sample code is the cadaver number followed by the day after placement.

Stage	Sample Code			
	36	47	50	67
Initial <i>CDH 0</i>	36-1	47-1	50-1	67-1
Bloat <i>CDH 410-250</i>	36-2 36-4	47-3 47-4	50-4	67-4 67-6 67-8
Bloat-Active <i>CDH 210-455</i>	36-6 36-8	47-5 47-6	50-5 50-6	67-10 67-13
Active <i>CDH 330-610</i>	36-10 36-12	47-7 47-8	50-8	67-17
Initial Advanced Decay <i>CDH 440-945</i>	36-14 36-16	47-9	50-10	67-23 67-29
Advanced Decay I <i>CDH 490-1785</i>	36-23	47-10 47-13	50-12 50-16	67-72
Advanced Decay II <i>CDH 1265-2455</i>	36-46	47-25 47-48	50-28 50-39	67-114
Advanced Decay III <i>CDH 3920-6515</i>	36-87	47-198	50-83	

VITA

Kelly Lynn Cobaugh was born in Fort Myers, Florida on October 27, 1988, moved to Michigan in 1997, and graduated from Farmington High School in 2007. Later that year, Kelly moved to Orlando, Florida and completed her Bachelor of Science in Microbiology and Molecular Biology from the University of Central Florida in 2011. Her undergraduate research project investigated the bactericidal effects of Auranofin on the pathogenic bacterium *Clostridium difficile* under the direction of Dr. William Self. In the fall of 2011 Kelly enrolled at the University of Tennessee to pursue a Master of Science degree in Environmental and Soil Science in the Biosystems Engineering and Soil Science department.